

Design and Optimization of Antenna Arrays for Beamforming and Radiation Pattern Control

Dimitrios Karatis, 10775, Electrical and Computer Engineering, AUTH

Abstract—This project explores the design and simulation of 2D antenna arrays using MATLAB, with a focus on radiation pattern calculation, directivity, and side lobe level optimization. The arrays are analyzed for various beam steering angles, and optimization methods, including genetic algorithms, are employed to minimize side lobe levels. Additionally, the mutual impedance and reflection coefficients of the arrays are computed to assess impedance matching. The results offer valuable insights into how array parameters influence antenna performance.

Index Terms—Antenna arrays, radiation patterns, side lobe level minimization, mutual impedance, reflection coefficient, dipole antennas, MATLAB simulation

I. INTRODUCTION

The primary objective of this project is to design and analyze 1D and 2D antenna arrays, focusing on their radiation patterns and beamforming capabilities. The design is simulated using MATLAB, and the effects of various parameters on the radiation pattern and array performance are evaluated.

The project is divided into several tasks:

- **2D Dipole Antenna Design:** We need to design and plot horizontal and vertical radiation patterns etc, for different steering angles and element spacings.
- **Directivity of Linearly Nonuniform Dipole Array:** We need to demonstrate the directivity of a linearly nonuniform array with different current distributions (both uniform and non-uniform), considering phase difference between adjacent elements.
- **Design of Nonuniform Dipole Array Using Optimization Techniques:** We need to minimize side lobes and maximize directivity using optimization methods, while comparing the results to those of a uniform array.
- **Input Impedance Calculation:** We need to calculate the mutual impedance and reflection coefficient of dipoles for different element spacings and configurations.

II. PROBLEM 1: 2D DIPOLE ANTENNA DESIGN

A. Horizontal and Vertical Radiation Patterns (1.1a)

We start by considering a 24×12 2D antenna array with element spacing $d = \lambda/2$. The goal is to calculate the horizontal and vertical radiation patterns for different beam angles, including zenith (θ_m) and azimuth (ϕ_m) angles.

The array factor AF for a uniform planar array is calculated as:

This document was prepared by Dimitrios Karatis as part of the second assignment for the Antennas and Propagation course at Aristotle University of Thessaloniki.

$$|AF_{xz}(\theta, \phi)| = \left| \frac{\sin\left(\frac{N_x \psi_x}{2}\right)}{\sin\left(\frac{\psi_x}{2}\right)} \right| \cdot \left| \frac{\sin\left(\frac{N_z \psi_z}{2}\right)}{\sin\left(\frac{\psi_z}{2}\right)} \right|$$

where:

$$\psi_x = kd_x \cos \phi \sin \theta + \delta_x$$

$$\psi_z = kd_z \cos \theta + \delta_z$$

with $k = \frac{2\pi}{\lambda}$ being the wave number, d_x and d_z are the element spacings in the x and z -directions respectively, and δ_x, δ_z are the phase shifts for beam steering.

Alternatively, the array factor can be expressed in product form:

$$|AF_{xz}(\theta, \phi)| = |AF_x(\psi_x)| \cdot |AF_z(\psi_z)| =$$

$$= \left| \sum_{m=0}^{N_x-1} \frac{I_{mx}}{I_{0x}} e^{jm\psi_x} \right| \cdot \left| \sum_{n=0}^{N_z-1} \frac{I_{nz}}{I_{0z}} e^{jn\psi_z} \right|$$

For uniform excitation with $I_{mx}/I_{0x} = 1$ and $I_{nz}/I_{0z} = 1$, this simplifies to the sinc-like form shown above, which I decided to use for this problem.

THEORETICAL ANALYSIS OF HORIZONTAL AND VERTICAL RADIATION PATTERNS

Horizontal Radiation Pattern

The horizontal radiation pattern is obtained by computing the electric field intensity E as a function of the azimuth angle ϕ for a fixed elevation angle $\theta = \pi/2$. The formula used to calculate the electric field is:

$$|E(\phi)| = |AF_{xz}(\phi)| \cdot |E_0|$$

where:

- $AF_{xz}(\phi)$ is the Array Factor, which describes the spatial distribution of the antenna array's radiation based on the positions and phase shifts of the individual elements.
- E_0 is the electric field intensity for a Hertzian dipole, which depends on the dipole's current, the wavelength, and the distance to the observation point.

$|E|$ is then normalized by its maximum value to allow for easier.

Vertical Radiation Pattern

The vertical radiation pattern is obtained similarly, but instead of varying the azimuth angle ϕ , we vary the elevation angle θ . The electric field is calculated as:

$$|E(\theta)| = |AF_{xz}(\theta)| \cdot |E_0|$$

where:

- $AF(\theta)$ is the Array Factor for the vertical pattern, describing how the array of dipoles radiates in the vertical direction.
- E_0 is the electric field intensity for a Hertzian dipole, similar to the horizontal case.

$|E|$ is then normalized by its maximum value, like before. In the Figure below we can see the horizontal as well as vertical radiation plots for the electric field intensity E_0 , of a Hertzian dipole.

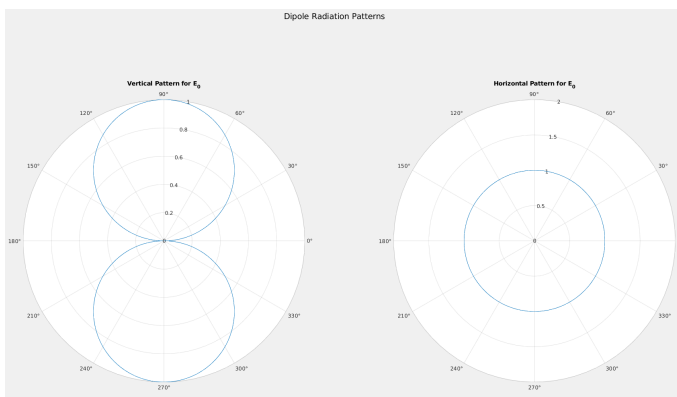


Fig. 1: Vertical and Horizontal Patterns for E_0

CALCULATION FOR SPECIFIC STEERING ANGLES

The next step is to calculate, in theory, the horizontal and vertical radiation patterns for some values of the beam steering angles θ_m and ϕ_m , in order to be able to validate the results of the simulation later on.

We start by the equations for ψ_x and ψ_z :

$$\psi_x = kd_x \cos \phi \sin \theta + \delta_x$$

$$\psi_z = kd_z \cos \theta + \delta_z$$

By substituting the equations for $k = \frac{2\pi}{\lambda}$ and $d_x = d_z = \lambda/2$, we have:

$$\psi_x = \pi \cos \phi \cdot \sin \theta + \delta_x$$

$$\psi_z = \pi \cos \theta + \delta_z$$

In order to achieve a maximum in the radiation pattern at specific angles, we need the phase shifts ψ_x and ψ_z to be zero.

The phase shifts δ_x and δ_z are computed as the difference between the actual phase terms and the required phase shifts for maximum radiation. Thus, they are given by:

$$\delta_x = \psi_x - \pi \cdot \cos(\phi) \cdot \sin(\theta)$$

$$\delta_z = \psi_z - \pi \cdot \cos(\theta)$$

Next, i will be calculating inidcative values for some of the cases:

1. For $(\theta_{\max}, \phi_{\max}) = (90^\circ, 60^\circ)$:

Since we want $\psi_x = 0$ and $\psi_z = 0$ for maximum radiation at $\theta_{\max} = 90^\circ$ and $\phi_{\max} = 60^\circ$, we substitute these values into the phase shift equations:

$$\delta_x = 0 - \pi \cdot \cos(\phi) \cdot \sin(\theta)$$

$$\delta_z = 0 - \pi \cdot \cos(\theta)$$

and we get:

$$\delta_x = -\frac{\pi}{2}$$

$$\delta_z = 0$$

Thus, for the case $(\theta_{\max}, \phi_{\max}) = (90^\circ, 60^\circ)$, the phase shifts are:

$$\delta_x(90^\circ, 60^\circ) = -\frac{\pi}{2}, \quad \delta_z(90^\circ, 60^\circ) = 0$$

2. For $(\theta_{\max}, \phi_{\max}) = (60^\circ, 30^\circ)$:

Since we want $\psi_x = 0$ and $\psi_z = 0$ for maximum radiation at $\theta_{\max} = 60^\circ$ and $\phi_{\max} = 30^\circ$, we substitute these values into the phase shift equations:

$$\delta_x = 0 - \pi \cdot \cos(\phi) \cdot \sin(\theta)$$

$$\delta_z = 0 - \pi \cdot \cos(\theta)$$

and we get:

$$\delta_x = -\frac{3\pi}{4}$$

$$\delta_z = -\frac{\pi}{2}$$

Thus, for the case $(\theta_{\max}, \phi_{\max}) = (60^\circ, 30^\circ)$, the phase shifts are:

$$\delta_x(60^\circ, 30^\circ) = -\frac{3\pi}{4}, \quad \delta_z(60^\circ, 30^\circ) = -\frac{\pi}{2}$$

Horizontal Radiation Pattern

For $\theta = \frac{\pi}{2}$ (zenith angle), the equations become:

$$\psi_x = \pi \cos \phi + \delta_x$$

$$\psi_z = \delta_z$$

- For $(\theta_{\max}, \phi_{\max}) = (90^\circ, 60^\circ)$

$$\psi_x = \pi \cos \phi \cdot \delta_x(90^\circ, 60^\circ) = \pi \cos \phi - \frac{\pi}{2}$$

$$\psi_z = \delta_z(90^\circ, 60^\circ) = 0$$

$\psi_x = 0$ for $\phi = 60^\circ \Rightarrow |A_x(\phi)|$ is going to be tilted towards the 60 degrees.

$\psi_z = 0 \Rightarrow |A_z(\phi)|$ plot is going to be a circle with radius N_z .

For a Hertzian dipole, the electric field E_0 at a distance r is given by:

$$E_0 = \frac{\eta_0 I_0 k l}{4\pi r} \sin(\theta)$$

Where:

- η_0 : Impedance of free space ($\approx 377 \Omega$)

- I_0 : Current amplitude

- k : Wave number ($k = \frac{2\pi}{\lambda}$)

- l : Dipole length

- r : Distance to observation point ($r \gg \lambda$)

- θ : Elevation angle

and so, for the horizontal plot ($\theta = 90^\circ$) we have that:

$$|E_0| = \left| \frac{\eta_0 I_0 k l}{4\pi r} \right|$$

which will just change the amplitude of the $|E|$ and not its direction.

Finally, the horizontal polar plot is going to be tilted towards the 60 degrees with an amplitude of $|E_0| \cdot |A_x(\phi)| \cdot |A_z(\phi)|$. Similar analysis can be conducted for the case of $(\theta_{\max}, \phi_{\max}) = (90^\circ, X)$

- For $(\theta_{\max}, \phi_{\max}) = (60^\circ, 30^\circ)$:

$$\psi_x = \pi \cos \phi + \delta_{x(60^\circ, 30^\circ)} = \pi \cos \phi - \frac{3\pi}{4}$$

$$\psi_z = \delta_{z(60^\circ, 30^\circ)} = -\frac{\pi}{2}$$

$\psi_x = 0$ for $\phi = \arccos(3/4) \approx 0.723$ rad, which is roughly $41.4^\circ \Rightarrow |A_x(\phi)|$ is going to be tilted towards the these degrees.

$\psi_z = -\frac{\pi}{2} \Rightarrow |A_z(\phi)| = 0$, from the known AF sine equation.

And so, the final horizontal radiation plot for this case is going to be zero, or it is going to be almost zero and on top of the 41.4 degrees, due to numerical approximation errors in MATLAB. Similar analysis can be conducted for the case of $(\theta_{\max}, \phi_{\max}) = (60^\circ, X)$

Vertical Radiation Pattern

For $\phi = \phi_{\max}$, the equations become:

$$\begin{cases} \psi_x = \delta_x, \\ \psi_z = \pi \cos(\theta) + \delta_z \quad \text{for } \phi_{\max} = 90^\circ \end{cases}$$

$$\begin{cases} \psi_x = \frac{\pi}{2} \sin(\theta) + \delta_x, \\ \psi_z = \pi \cos(\theta) + \delta_z \quad \text{for } \phi_{\max} = 60^\circ \end{cases}$$

$$\begin{cases} \psi_x = \frac{\pi\sqrt{3}}{2} \sin(\theta) + \delta_x, \\ \psi_z = \pi \cos(\theta) + \delta_z \quad \text{for } \phi_{\max} = 30^\circ \end{cases}$$

And so,

- For $(\theta_{\max}, \phi_{\max}) = (90^\circ, 60^\circ)$:

$$\psi_x = \frac{\pi}{2} \sin(\theta) + \delta_{x(90^\circ, 60^\circ)} = \frac{\pi}{2} \sin(\theta) - \frac{\pi}{2}$$

$$\psi_z = \pi \cos(\theta) - 0 = \pi \cos(\theta)$$

$\psi_x = 0 = \psi_z$ for $\theta = 90^\circ$ and so, using the same analysis as before we get a lobe at 90° . This time tho, it is important to note that the E_0 is not a circle centered at zero, as shown in Figure 1. Since we can see that the 90 degrees are well within the circle and with a reasonably high amplitude, it is safe to say that we expect the plot to be pointing at the 90 degree mark. A similar analysis can be applied for other cases, such as $(\theta_{\max}, \phi_{\max}) = (90^\circ, X^\circ)$ and $(60^\circ, X^\circ)$. In the latter case, when $\theta = 60^\circ$, the radiation pattern is expected to peak around 60° .

PLOT RESULTS AND DISCUSSION

Next, I am going to present the radiation patterns for both horizontal and vertical polarizations, comparing the cases with and without normalization.

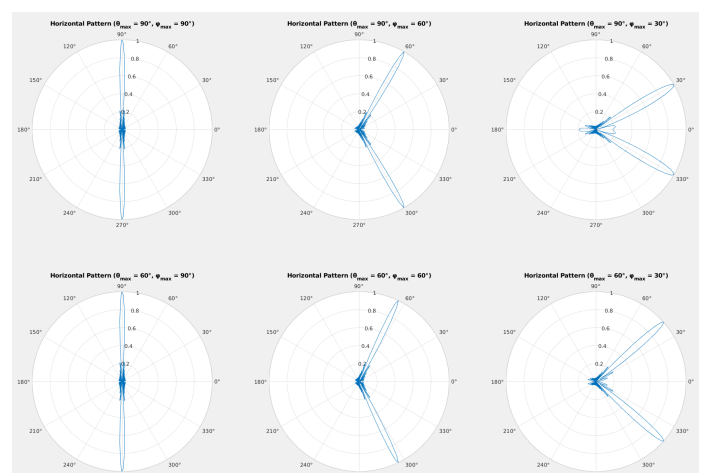


Fig. 2: Horizontal Radiation Plots (Normalized)

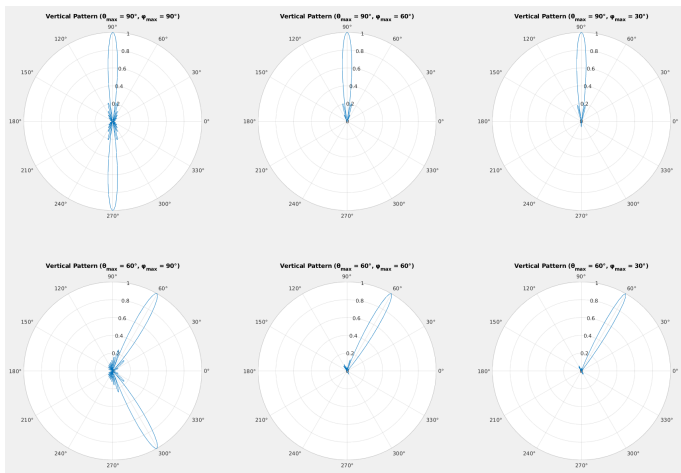


Fig. 3: Vertical Radiation Plots (Normalized)

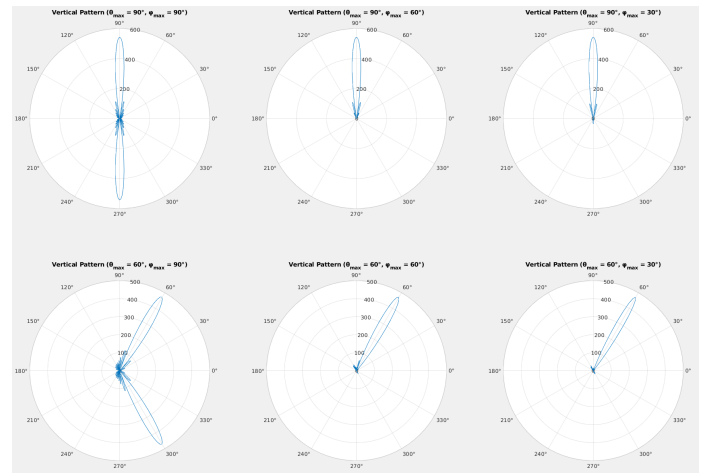


Fig. 5: Vertical Radiation Plots (Not Normalized)

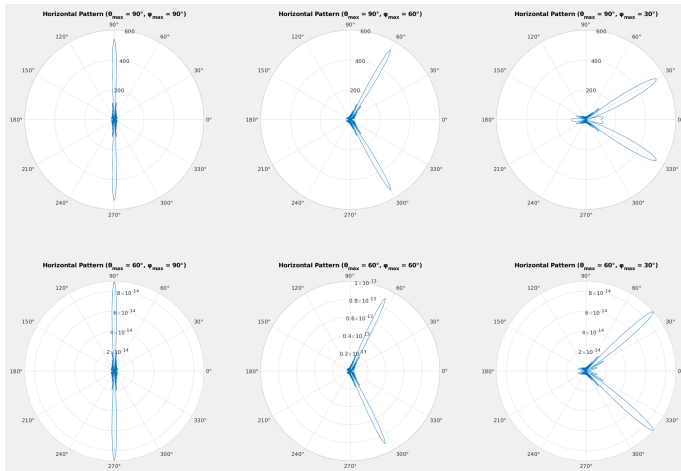


Fig. 4: Horizontal Radiation Plots (Not Normalized)

From Figures 2 to 5, we can observe that the theoretical analysis closely matches the results shown by the plots. For the horizontal radiation patterns, it is evident that when $(\theta_{\max}, \phi_{\max}) = (90^\circ, X^\circ)$, the main lobe is directed towards the X° direction. In contrast, when $(\theta_{\max}, \phi_{\max}) = (60^\circ, X^\circ)$, the radiation pattern is essentially zero, though it doesn't exactly seem zero at the not normalized plots due to numerical approximations performed by MATLAB.

Finally, for the vertical radiation patterns, the theoretical analysis also holds true. When $(\theta_{\max}, \phi_{\max}) = (90^\circ, X^\circ)$, the main lobe is directed towards the 90° mark, and when $(\theta_{\max}, \phi_{\max}) = (60^\circ, X^\circ)$, it faces the 60° one, exactly as predicted by the analysis above. Also, note that the analysis for the vertical patterns above was conducted only for one half of the plane. Therefore, for all cases it is necessary to consider the other half of the plane as well. And so, for example, for the $(\theta_{\max}, \phi_{\max}) = (90^\circ, 60^\circ)$ case we have:

$$\phi = \phi_{\max} + 180^\circ = 240^\circ \text{ (rear hemisphere), so:}$$

$$\psi_x = \pi \cos \phi \sin \theta - \frac{\pi}{2} = -\frac{\pi}{2} \sin \theta - \frac{\pi}{2}$$

Thus, the visible region of ψ_x is:

$$-\pi \leq \psi_x \leq -\frac{\pi}{2}$$

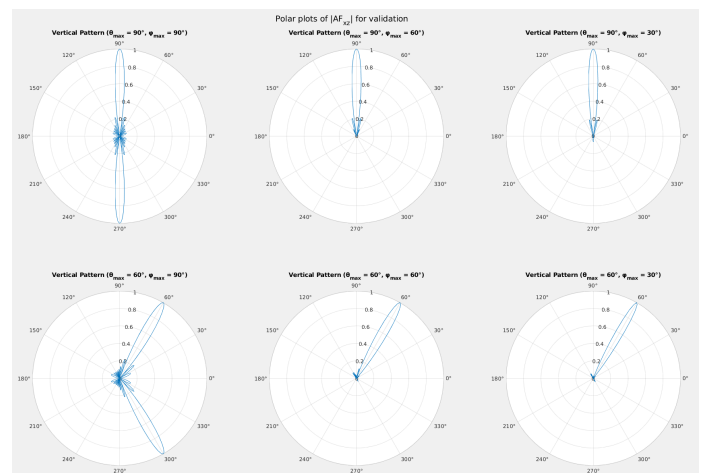
which corresponds to the side lobe region. Therefore, for that case, in the rear hemisphere, we only observe side lobes. A similar analysis can be performed for the other cases, which validates the vertical plot results.

In order to further validate the amplitude of the computed electric field intensity, I decided to compare it to the product of the maximum electric field (E_0) and the Array Factor (AF). The relationship is given by:

$$|E| = |E_0| \cdot |AF_{xz}|$$

And so, additional code was created that plots:

- The field intensity E_0 (Figure 1) for both horizontal and vertical radiation patterns.
- The array factor $|AF_{xz}|$ (Figure 6) for just the vertical case.

Fig. 6: Vertical Polar Plots for $|AF_{xz}|$

By examining their relations, it is safe to say that the given horizontal and vertical radiation plots (Figures 2 to 5) of the

2D antenna are correct.

Detailed code can be found in the `antennas_1_1a.m` MATLAB file.

B. 3D Radiation Patterns (1.1b)

The following steps were implemented in MATLAB to generate the required 3D surface plots for all combinations of $\theta_m \in \{90^\circ, 60^\circ\}$ and $\phi_m \in \{90^\circ, 60^\circ, 30^\circ\}$, based on the logic of the previous question (1.1a).

- 1) **Grid Definition:** A fine mesh grid was created for the full angular domain ($0 \leq \theta \leq 180^\circ$ and $0 \leq \phi \leq 360^\circ$) using `meshgrid` with 180×360 points.
- 2) **Phase Shift Calculation (δ_x, δ_z):** For each combination of steering angles (θ_m, ϕ_m) , the static phase shifts δ_x and δ_z were calculated using the formulas derived from the maximum direction requirement.
- 3) **Total Field Calculation:** The total Array Factor magnitude (AF_{abs}) was calculated over the entire (θ, ϕ) grid by multiplying the individual AF_x and AF_z magnitudes. The total electric field magnitude (E_{abs}) was then found by multiplying the AF_{abs} by the element factor term ($|E_0|$), and the result was normalized (E_{abs_norm}) to its peak value.
- 4) **Coordinate Transformation:** To plot the radiation pattern as a 3D surface, the normalized field values (acting as the radial distance, r) were converted from spherical coordinates (r, θ, ϕ) to Cartesian coordinates (X, Y, Z) :

$$X = E_{abs_norm} \cdot \sin \theta \cdot \cos \phi$$

$$Y = E_{abs_norm} \cdot \sin \theta \cdot \sin \phi$$

$$Z = E_{abs_norm} \cdot \cos \theta$$

- 5) **Surface Visualization:** The `surf` function was used to generate the 3D plot, where the normalized electric field intensity (E_{abs_norm}) was also used to color-code the surface, allowing for a clear visual representation of the main beam and side lobe intensity distribution in space.

The corresponding plots can be seen below.

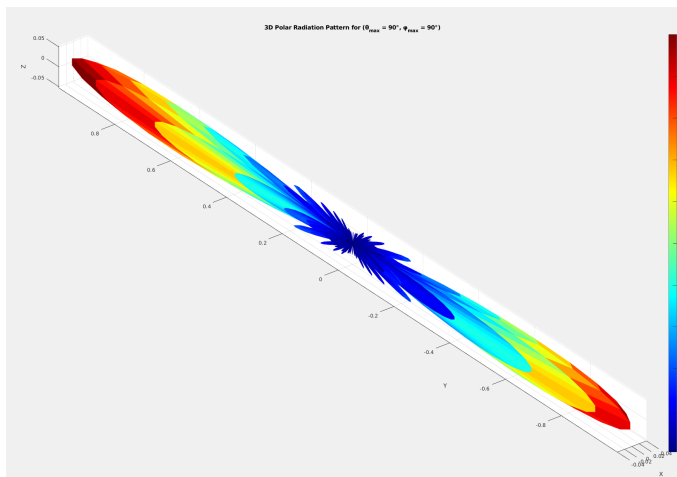


Fig. 7: 3D Polar Radiation Pattern for $(\theta_{max}, \phi_{max}) = (90^\circ, 90^\circ)$.

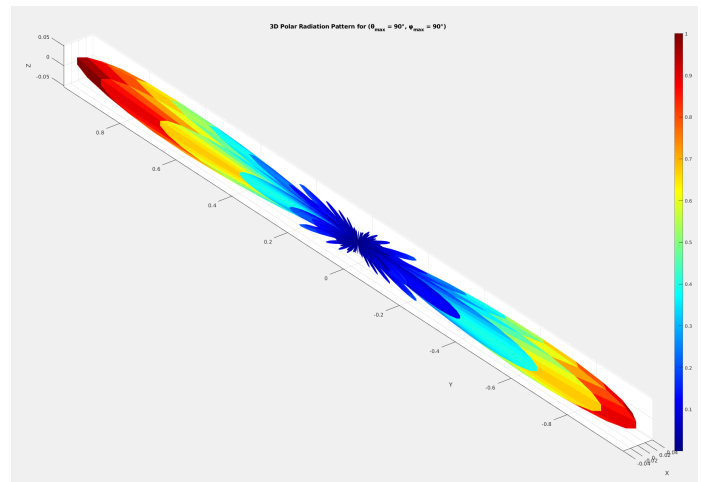


Fig. 8: 3D Polar Radiation Pattern for $(\theta_{max}, \phi_{max}) = (90^\circ, 90^\circ)$.

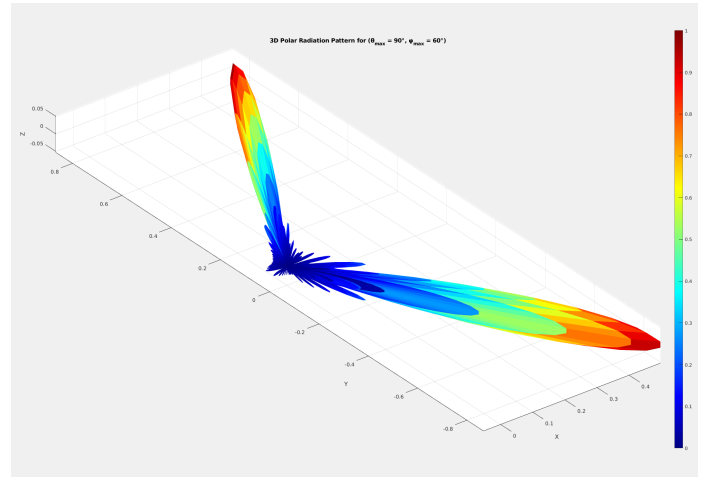


Fig. 9: 3D Polar Radiation Pattern for $(\theta_{max}, \phi_{max}) = (90^\circ, 60^\circ)$.

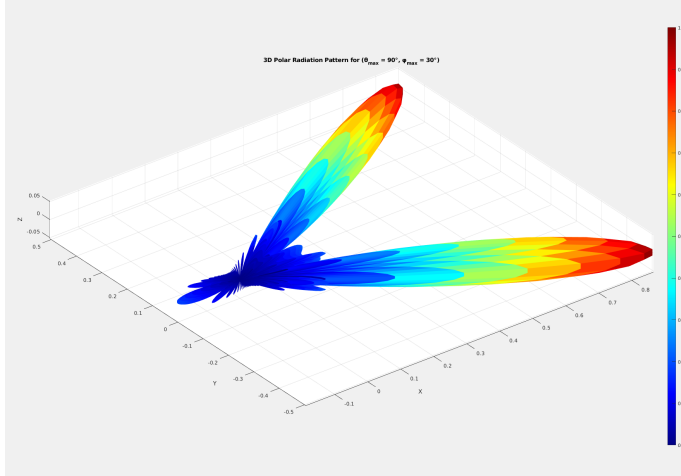


Fig. 10: 3D Polar Radiation Pattern for $(\theta_{\max}, \phi_{\max}) = (90^\circ, 30^\circ)$.

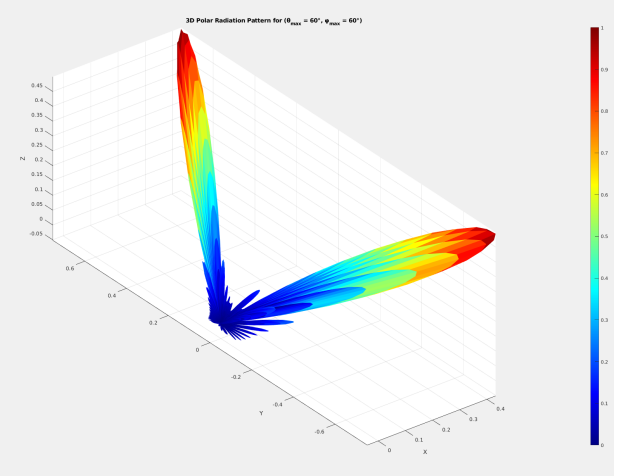


Fig. 12: 3D Polar Radiation Pattern for $(\theta_{\max}, \phi_{\max}) = (60^\circ, 60^\circ)$.

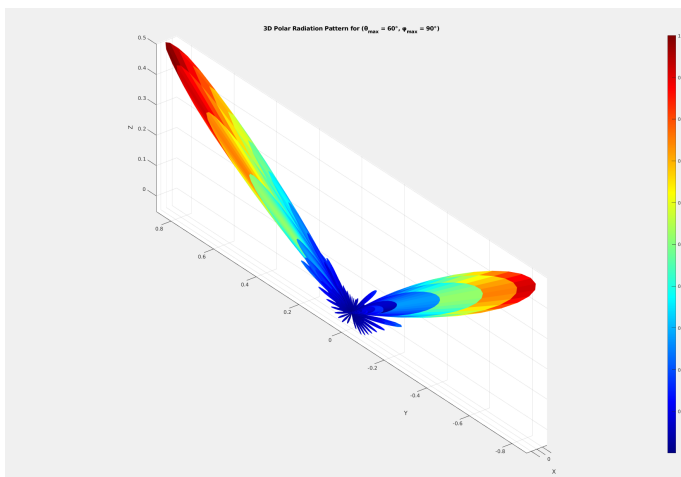


Fig. 11: 3D Polar Radiation Pattern for $(\theta_{\max}, \phi_{\max}) = (60^\circ, 90^\circ)$.

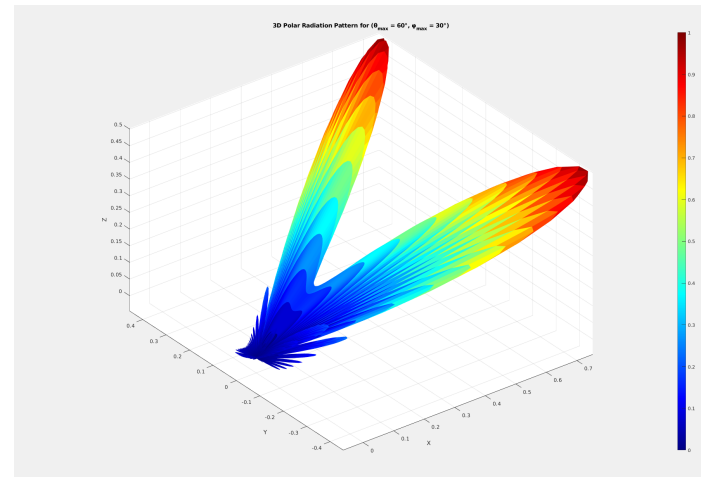


Fig. 13: 3D Polar Radiation Pattern for $(\theta_{\max}, \phi_{\max}) = (60^\circ, 30^\circ)$.

Detailed code can be found in the `antennas_1_1b.m` MATLAB file.

C. Directivity calculation of the antenna (1.1c)

Next we need to calculate the total directive gain (D) of the array antenna for the 6 different $(\theta_{\max}, \phi_{\max})$ cases.

For this reason, two independent methods were used to estimate the total directivity:

- 1) **Method 1:** Utilizing the theoretical linear array directivity formula for uniform arrays, involving the Sine Integral ($\text{Si}(x)$).
- 2) **Method 2:** Using the Half-Power Beamwidth (HPBW) approximation formula.

Coordinate System Transformation

Since the dipole elements are aligned along the x, z axis and the formulas work by having them on the x, y plane, a change of coordinates is necessary. In this new system:

- The new x' -axis aligns with the original z -axis.

- The new y' -axis aligns with the original x -axis.

The spherical coordinates in the original system are:

$$x = r \sin(\theta) \cos(\phi)$$

$$y = r \sin(\theta) \sin(\phi)$$

$$z = r \cos(\theta)$$

- **New Elevation Angle (θ'_0):** The new elevation angle is given by:

$$\theta'_0 = \arccos\left(\frac{z}{r}\right) = \arccos(\cos(\theta)) = \arccos(\sin(\theta) \sin(\phi))$$

- **New Azimuth Angle (ϕ'_0):** The new azimuth angle is given by:

$$\phi'_0 = \arctan_2\left(\frac{y}{x}\right) = \arctan_2\left(\frac{\sin(\theta) \sin(\phi)}{\sin(\theta) \cos(\phi)}\right) = \arctan_2(\sin(\theta) \cos(\phi), \cos(\theta))$$

Thus, the final transformation formulas are:

$$\begin{aligned}\theta'_0 &= \arccos(\sin(\theta) \sin(\phi)) \\ \phi'_0 &= \arctan_2(\sin(\theta) \cos(\phi), \cos(\theta))\end{aligned}$$

The results of these transformations are summarized in the Tables below.

Initial (θ, ϕ) (deg)	New (θ'_0, ϕ'_0) (deg)	Deviation from broadside in $x(y')$	Deviation from broadside in $z(x')$
(90, 90)	(0, 90)	0°	0°
(90, 60)	(30, 90)	30°	0°
(90, 30)	(60, 90)	60°	0°
(60, 90)	(30, 0)	0°	30°
(60, 60)	(41.41, 40.89)	41.41°	49.11°
(60, 30)	(64.34, 56.31)	64.34°	33.69°

TABLE I: Coordinate System Transformation and Deviation from Broadside

Initial (θ, ϕ) (deg)	New (θ'_0, ϕ'_0) (deg)	Broadside $x(y')$	Broadside $z(x')$
(90, 90)	(0, 90)	YES	YES
(90, 60)	(30, 90)	CONS	YES
(90, 30)	(60, 90)	CONS	YES
(60, 90)	(30, 0)	YES	CONS
(60, 60)	(41.41, 40.89)	CONS	CONS
(60, 30)	(64.34, 56.31)	NO	CONS

TABLE II: Coordinate System Transformation and Broadside Results. **YES** means that it is truly a broadside case, **CONS** means that it can be considered as broadside for simplicity, while **NO** means that it cannot be considered as broadside at all.

Keep in mind that we consider an antenna broadside if its deviation is $\leq 60^\circ$. So, for the most part, all cases can be treated as broadside, except for the antenna at $x(y')$ with angles $(\theta_{\max}, \phi_{\max}) = (60^\circ, 30^\circ)$. For that case, tho, I still used the broadside array formulas, for comparison reasons.

Directivity Calculation Formulas

1) **Method 1: Sine Integral Method (Using Linear Array Directivity D_{linear}):** For this method the formula that was used was:

$$D_{\text{total}} \approx \pi \cdot \cos(\theta'_0) \cdot D_x \cdot D_z$$

For the D_x and D_z , in cases where the antenna is broadside with zero deviation, they were calculated using the standard equation ($D = 2Nd/\lambda$). The MATLAB code includes specific adjustments for D_x and D_z in non-broadside cases by dividing the broadside directivity by an estimated HPBW ratio to account for steering loss. So, in cases where there is deviation from broadside, the formula used was:

$$D_{\theta'_0} \approx \frac{D_0 \text{HPBW}_0}{\text{HPBW}_{\theta'_0}}$$

where HPBW_0 (for the broadside case) and $\text{HPBW}_{\theta'_0}$ can be calculated from the Array Length diagram in Figure 14 (also see the tables below). Finally, remember that this equation doesn't apply if the deviation from broadside is greater than 60 degrees, which means that the results for the last case $(\theta, \phi) = (60^\circ, 30^\circ)$ for the $x(y')$ are not very accurate.

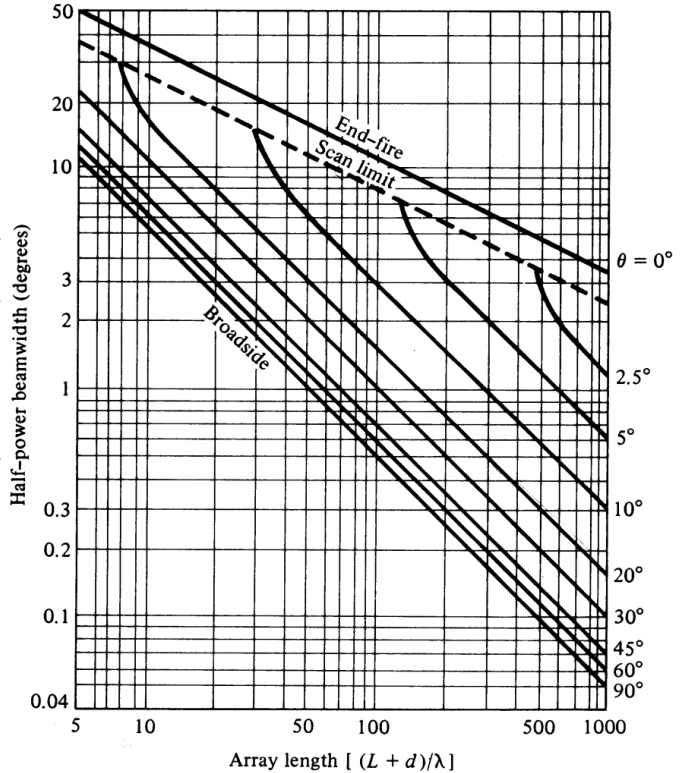


Fig. 14: The Array Length diagram.

2) **Method 2: HPBW Approximation Method:** The total directivity is estimated using the effective half-power beamwidths (Θ_h and Ψ_h) in the direction of maximum radiation:

$$D_{\text{total}} \approx \frac{32400}{\Theta_h \cdot \Psi_h}$$

The effective beamwidths are given by:

$$\Theta_h = \frac{1}{\cos(\theta'_0) \sqrt{\frac{\cos^2(\phi'_0)}{\Theta_{x'}^2} + \frac{\sin^2(\phi'_0)}{\Theta_{z'}^2}}} \quad \text{and} \quad \Psi_h = \frac{1}{\sqrt{\frac{\cos^2(\phi'_0)}{\Theta_{z'}^2} + \frac{\sin^2(\phi'_0)}{\Theta_{x'}^2}}}$$

The manually set HPBW values used in both methods are shown in Table III.

Initial (θ, ϕ) (deg)	Steered Θ_x (deg)	Steered Θ_z (deg)
(90.0, 90.0)	4.8° (Broadside)	9° (Broadside)
(90.0, 60.0)	5.4°	9° (Broadside)
(90.0, 30.0)	9.5°	9° (Broadside)
(60.0, 90.0)	4.8° (Broadside)	10.5°
(60.0, 60.0)	6.7°	14.0°
(60.0, 30.0)	12.5°	11.5°

TABLE III: Manual HPBW Values Used for Steered Beams (degrees)

Numerical Results and Analysis

The calculated directivity results are summarized in Table IV.

1) **Maximum Directivity (Broadside):** The maximum directivity is achieved at the broadside direction, $(\theta, \phi) = (90^\circ, 90^\circ)$.

Initial (θ, ϕ) (deg)	Method 1 (D_x, D_z)	Method 2 (D_{HPBW})	Difference
(90.0, 90.0)	29.565	28.751	0.814
(90.0, 60.0)	28.429	27.614	0.815
(90.0, 30.0)	23.590	22.775	0.815
(60.0, 90.0)	28.271	27.456	0.815
(60.0, 60.0)	24.949	25.202	0.253
(60.0, 30.0)	20.709	19.907	0.802

TABLE IV: Directivity Results Comparison (dBi)

- 2) **Steering Loss and Beam Broadening:** As the beam is steered away from broadside, the directivity drops significantly. The most extreme steering case, $(\theta, \phi) = (60^\circ, 30^\circ)$, results in a directivity of approximately 20 dBi, corresponding to a 8 dB loss.
- 3) **Method Consistency:** Both methods show strong agreement, with results differing by up to 0.8 dBi. Also, for five out of the six cases, Method 1 yields a directivity value that is higher compared to Method 2. Only in the 5th case ($(\theta_{\max}, \phi_{\max}) = (60^\circ, 60^\circ)$), Method 2's results were higher than Method 1's. The small discrepancies between the methods were likely amplified by the approximations that were made when it comes to choosing values from the Array Length diagram and also the approximations each equation used in order to be derived.

Lastly, we need to keep in mind that one of these calculations used formulas for broadside when in fact the deviation was more than 60 degrees from it ($(\theta_{\max}, \phi_{\max}) = (60^\circ, 30^\circ)$).

In conclusion, the 24×12 planar array seems to demonstrate high gain at broadside, which systematically decreases due to the element pattern and beam broadening effects being steered away from the broadside region.

Detailed code can be found in the `antennas_1_1c.m` MATLAB file.

D. Theoretical Calculation of Directivity (Riemann Sum) (1.1d)

The directivity (D) of an antenna is defined as the ratio of the maximum radiation intensity (U_{\max}) to the total average radiated power (P_{rad}):

$$D = \frac{4\pi U_{\max}}{P_{\text{rad}}}$$

The total radiated power (P_{rad}) is found by integrating the radiation intensity (U) over all solid angles:

$$P_{\text{rad}} = \iint_{4\pi} U(\theta, \phi) d\Omega = \int_0^{2\pi} \int_0^\pi U(\theta, \phi) \sin \theta d\theta d\phi$$

The radiation intensity $U(\theta, \phi)$ is proportional to the magnitude squared of the electric field ($|E|^2$), which in this case includes both the Element Factor and the Array Factor (AF) as we said in the previous questions: $|E|^2 = |AF_{xz}|^2 \cdot |E_0|^2$.

Computational Methodology (Riemann Sum)

The integral for P_{rad} was calculated numerically using the Riemann Sum approximation over a dense computational grid.

- 1) **Grid Setup:** A dense grid was established using 180 points for the zenith angle θ (from 0 to π) and 360 points for the azimuth angle ϕ (from 0 to 2π). The step sizes $d\theta$ and $d\phi$ were calculated from these points.
- 2) **Radiation Intensity Calculation (U):** For each point (θ, ϕ) on the grid, the normalized radiation intensity U was calculated:

$$U(\theta, \phi) = |E|^2 = |\text{AF}_x \cdot \text{AF}_z \cdot E_0|^2$$

where $\text{AF}_x = \frac{\sin(N_x \Psi_x/2)}{\sin(\Psi_x/2)}$, $\Psi_x = kd \sin \theta \cos \phi + \delta_x$

- 3) **Numerical Integration:** The total radiated power P_{rad} was approximated by summing the radiation intensity at each grid point, weighted by the element $\sin \theta d\theta d\phi$:

$$P_{\text{rad}} \approx \sum_{\phi} \sum_{\theta} U(\theta, \phi) \sin \theta \cdot d\theta \cdot d\phi$$

- 4) **Directivity Calculation:** The final directivity D was computed by taking the ratio of the maximum intensity found on the grid ($U_{\max} = \max(U)$) to the calculated total radiated power P_{rad} .

Numerical Results and Analysis

The directivity was calculated for all specified combinations of maximum radiation angles (θ_m, ϕ_m) .

TABLE V: Directivity Calculated Numerically via Riemann Sum (1.1d)

θ_m (deg)	ϕ_m (deg)	D (Linear)	D (dBi)
90.0	90.0	444.6831	26.48
90.0	60.0	385.3064	25.86
90.0	30.0	211.4325	23.25
60.0	90.0	390.5325	25.92
60.0	60.0	338.8446	25.30
60.0	30.0	195.4764	22.91

The results demonstrate the expected phenomenon of scanning loss:

- **Maximum Directivity:** The highest directivity ($D = 444.68$) is achieved when the beam is pointed to the broadside direction ($\theta_m = 90^\circ, \phi_m = 90^\circ$), where the Element Factor (E_0) is maximized and the Array Factor aligns perfectly.
- **Beam Scanning Loss:** When the beam is steered away from broadside (e.g., to $\theta_m = 60^\circ$ or $\phi_m = 30^\circ$), the directivity decreases (e.g., down to $D = 195.48$ for $\theta_m = 60^\circ, \phi_m = 30^\circ$).

Comparative Analysis of Directivity Methods

Numerical Results (Riemann Sum)

The Riemann Sum approximation method is considered the most accurate, as it avoids the simplifying assumptions inherent in 1.1c methods. In order to assess the accuracy of the all the directivity methods used both in 1.1c and in 1.1d, all results are gathered in Table VI.

Initial (θ, ϕ) (deg)	Riemann	Method 2 (D_{HPBW})	Method 1 (D_x, D_z)
(90.0, 90.0)	26.48	28.751	29.565
(90.0, 60.0)	25.86	27.614	28.429
(90.0, 30.0)	23.25	22.775	23.590
(60.0, 90.0)	25.92	27.456	28.271
(60.0, 60.0)	25.30	25.202	24.949
(60.0, 30.0)	22.91	19.907	20.709

TABLE VI: Directivity Results from All Three Calculation Methods (dBi)

Initial (θ, ϕ) (deg)	Riemann	Method 2 (D_{HPBW})	Difference
(90.0, 90.0)	26.48	28.751	2.271
(90.0, 60.0)	25.86	27.614	1.754
(90.0, 30.0)	23.25	22.775	0.475
(60.0, 90.0)	25.92	27.456	1.536
(60.0, 60.0)	25.30	25.202	0.098
(60.0, 30.0)	22.91	19.907	3.003

TABLE VII: Directivity Comparison between Riemann and HPBW Methods (dBi)

a) Method Accuracy: The Numerical Integration

Method (1.1d) is the most accurate approach as it is based on the fundamental definition of directivity: $D = 4\pi U_{\max}/P_{\text{rad}}$. It directly computes the total radiated power (P_{rad}) by integrating the radiation intensity (U) over the entire sphere, avoiding approximations. Next up follows the HPBW method with differences from nearly zero to 3 dBi.

b) Overestimation at Broadside: For the true broadside case, $(\theta, \phi) = (90^\circ, 90^\circ)$, as well as in other cases, the two approximation methods in 1.1c yield results that are approximately 1 – 3 dBi higher than the accurate numerical results. The primary reason for these overestimations lies in the approximations used in both Methods 1 and 2 and also in the Array Length diagram values, as discussed in the previous question.

However, for the third and fifth case, $(\theta, \phi) = (90^\circ, 30^\circ)$ and $(\theta, \phi) = (60^\circ, 60^\circ)$, the approximation methods showed very good agreement (22.775 and 25.202 dBi) with the numerical results (23.25 dBi and 25.30 dBi).

c) Steering Loss Trends and Errors: All three methods correctly demonstrated the phenomenon of **scanning loss**: the directivity consistently decreases as the beam is steered away from broadside.

Detailed code can be found in the `antennas_1_Id.m` MATLAB file.

E. End-Fire Operation and Directivity Analysis (1.1e)

The objective was to configure the 24×12 planar array to operate in end-fire mode with the maximum radiation steered along the positive x -axis ($\theta_m = 90^\circ, \phi_m = 0^\circ$). Since the elements are spaced at $d = \lambda/2$, achieving ideal end-fire requires a specific progressive phase shift $\delta = -kd$.

- **Steering Angles:** The target direction is the x -axis: $\theta_m = \pi/2$ (90°) and $\phi_m = 0$ (0°).
- **Required Phase Shifts (δ_x, δ_z):**

$$\delta_x = -kd \sin \theta_m \cos \phi_m = -k(\lambda/2) \sin(\pi/2) \cos(0) = -\pi$$

$$\delta_z = -kd \cos \theta_m = -k(\lambda/2) \cos(\pi/2) = 0$$

Directivity Calculation and Comparison

Three methods were used to calculate the directivity (D).

Method 1: Riemann Sum (Definition Method): This method is the most reliable as it calculates the directivity based on its fundamental definition, $D = 4\pi U_{\max}/P_{\text{rad}}$, using the calculated $U(\theta, \phi)$ over the grid:

- U_{\max} is the maximum radiation intensity found on the computational grid.
- P_{rad} is the total radiated power computed via the **Riemann Sum** of $U(\theta, \phi) \sin \theta d\theta d\phi$.
- **Result:** The calculated directivity is **18.714** dBi. This value represents the true directivity of the resulting end-fire pattern.

Method 2: $D_x D_z$ Formula: This method attempts to use the simplified directivity formula often derived for uniform broadside arrays, adapted for planar arrays as $D = \pi D_x D_z \cos \theta'_0$. Since we need $(\theta_m, \phi_m) = (90^\circ, 0^\circ)$ in order to have end-fire along x axis, then from the transformation of the coordinate system we have $\theta'_0 = 90^\circ$ and $\phi'_0 = 90^\circ$ and so $\cos \theta'_0 = 0$. That means that this formula cannot be used for end-fire cases and is therefore discarded from the analysis.

Method 3: HPBW Formula: This method uses the HPBW formula, which is explicitly designed for end-fire patterns, estimating directivity from the Half-Power BeamWidth (HPBW): $D \approx 32400/(\Theta_x \Theta_z)$.

- The code uses the HPBW formula specific to end-fire arrays ($\Theta_x = 105.4^\circ \sqrt{\lambda/(N_x d)}$) for the x -direction and the broadside HPBW for the z -direction ($\Theta_z = 48.4^\circ \frac{\lambda}{Nd}$). Alternatively we could take these values from the Array Length diagram (Fig. 14), as we did in 1.1c.
- **Result:** The calculated directivity is **21.206** dBi. This is the typical result expected from the HPBW approximation for end-fire arrays, which is often an overestimate.

Method	Formula Dependence	Result (dBi)
Riemann Sum	$D = 4\pi U_{\max}/P_{\text{rad}}$	18.714
Linear Array	$D = \cos \theta'_0 \cdot D_x \cdot D_z$	(Cannot be used)
HPBW Approximation	$D = 32400/(\Theta_x \Theta_z)$	21.206

TABLE VIII: Directivity Comparison for End-Fire ($\theta_m = 90^\circ, \phi_m = 0^\circ$)

Below we can also see the 3D Radiation Pattern for that case.

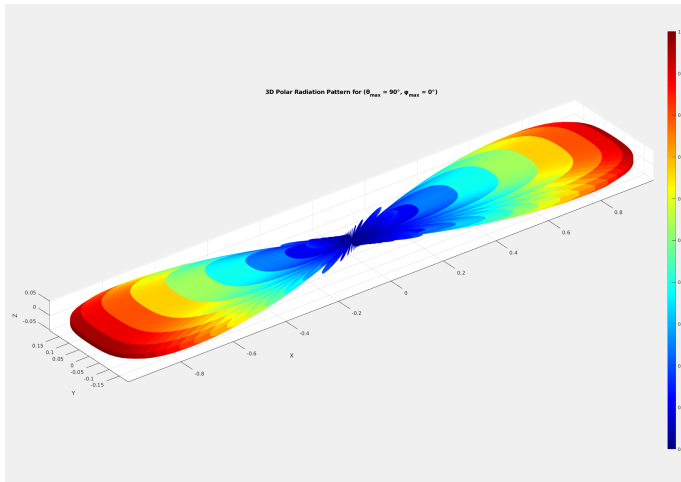


Fig. 15: 3D Polar Radiation Pattern for the End-Fire case.

Detailed code can be found in the antennas_1_1e.m MATLAB file.

F. Hansen-Woodyard End-Fire Operation and Directivity (1.1st)

The objective was to design the 24×12 planar array to operate under the Hansen-Woodyard condition along the positive x -axis ($\theta_m = 90^\circ, \phi_m = 0^\circ$). This method uses a specific phase shift slightly larger (in absolute value) than the standard end-fire phase shift ($\delta = -kd$) to boost directivity, though it makes the pattern extremely sensitive to frequency variations.

- **Steering Direction:** x -axis ($\theta_m = 90^\circ, \phi_m = 0^\circ$).
- **Hansen-Woodyard Phase Shift (δ_x):** The required progressive phase shift for the axis of radiation is:

$$\delta_x = -kd - \frac{2.92}{N_x}$$

where $N_x = 24$ and $d = \lambda/2$, so $kd = \pi$.

- **Transverse Phase Shift (δ_z):** The array is broadside in the z -direction: $\delta_z = 0$.

Directivity Calculation and Comparison

The directivity was calculated using three distinct methods: numerical integration, a specialized analytical formula, and the HPBW approximation.

Method 1: Riemann Sum (Definition Method): The numerical calculation of directivity (Riemann Sum, $D = 4\pi U_{\max}/P_{\text{rad}}$) again is the most accurate method, as it accounts for the actual pattern shape generated by the H-W phase shift.

- U_{\max} is the maximum intensity found on the grid, and P_{rad} is the total radiated power computed via the Riemann Sum approximation ($\sum U \sin \theta d\theta d\phi$).
- **Result:** The calculated directivity is **20.019** dBi. This value represents the true directivity of the resulting H-W pattern. (Compared to the 18.714 dBi obtained in the standard end-fire case (Problem 1.1e), the H-W condition successfully provided a boost of ≈ 1.3 dBi).

Method 2: (Hansen-Woodyard Formula): As noted in Problem 1.1(e), the analytical formula $D_{\text{total}} = \pi D_x D_z \cos \theta'_0$ cannot be used in the end-fire case since it yields 0 and so once again is discarded from the analysis.

Method 3: HPBW Approximation: This method approximates directivity using the product of the HPBWs in the orthogonal planes. Specialized H-W formulas are used for the end-fire HPBW (Θ_x) and the broadside HPBW for the z -axis (Θ_z), where

$$\Theta_z = 48.4^\circ \frac{\lambda}{Nd}$$

and

$$\Theta_x = 2\cos^{-1}(1 - 0.1398) \frac{\lambda}{Nd}$$

- The planar directivity is estimated as: $D_{\text{HPBW}} = 32400 / (\Theta_x \cdot \Theta_z)$.
- **Result:** The calculated directivity is **23.606** dBi. This value is higher than the numerical result, confirming that HPBW approximations tend to overestimate directivity.

Method	Result (dBi)
Riemann Sum	20.019
Linear Array	(Cannot be used)
HPBW Approximation	23.606

TABLE IX: Directivity Comparison for Hansen-Woodyard End-Fire ($\theta_m = 90^\circ, \phi_m = 0^\circ$)

Finally, in all cases, we observe that the directivity of the H-W antenna is higher compared to the end-fire antenna (as discussed in the previous question). Also, below we can see the 3D radiation pattern for this case, where we observe an increase in directivity, but a deterioration in the main-to-side lobe ratio, just like the theory suggests.

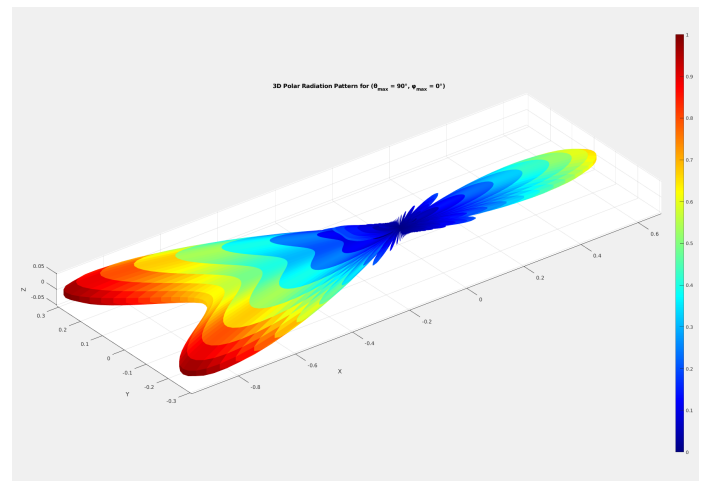


Fig. 16: 3D Polar Radiation Pattern for the Hansen-Woodyard case.

Detailed code can be found in the antennas_1_1st.m MATLAB file.

III. PROBLEM 2: DIRECTIVITY OF LINEARLY NONUNIFORM DIPOLE ARRAY

INTRODUCTION AND PROBLEM STATEMENT

A linear non-uniform array of N elements ($n = 0, 1, \dots, N-1$), spaced by a distance d and having real and positive current amplitudes I_0, I_1, \dots, I_{N-1} but a constant phase difference δ between successive currents, is a generalization of the uniform array.

The complex current of the n -th element is $I_n e^{jn\delta}$. We assume isotropic elements $|E_0| = \text{const}$ and equal to 1. We aim to prove that the directivity D is given by the expression:

$$D = \frac{kd \left(\sum_{n=0}^{N-1} I_n \right)^2}{\sum_{n=0}^{N-1} \sum_{m=0}^{N-1} I_n I_m e^{j(n-m)\delta} \frac{\sin[(n-m)kd]}{n-m}}$$

PROOF

The Directivity D is defined as the ratio of the maximum radiation intensity (U_{\max}) to the average radiation intensity (U_{avg}) over the entire sphere:

$$D = \frac{4\pi U_{\max}}{P_{\text{rad}}} = \frac{4\pi |AF|_{\max}^2}{P_{\text{rad}}}$$

where P_{rad} is the total radiated power, $\int_0^{2\pi} \int_0^\pi |AF(\psi)|^2 \sin \theta d\theta d\phi$. Keep in mind that this is a simplified version for $|E_0| = 1$.

A. Calculation of the Numerator (Maximum Array Factor)

The maximum Array Factor (AF_{\max}) occurs when the total phase difference $\psi = kd \cos \theta + \delta$ is zero. The maximum is therefore:

$$|AF|_{\max} = \left| \sum_{n=0}^{N-1} I_n e^{jn\psi} \right|_{\psi=0} = \sum_{n=0}^{N-1} I_n$$

and so, the numerator is:

$$4\pi |AF|_{\max}^2 = 4\pi \left(\sum_{n=0}^{N-1} I_n \right)^2$$

B. Calculation of the Denominator (Total Radiated Power P_{rad})

The Array Factor squared is found by multiplying AF by its conjugate:

$$|AF|^2 = \left(\sum_{n=0}^{N-1} I_n e^{jn\psi} \right) \left(\sum_{m=0}^{N-1} I_m e^{-jm\psi} \right) = \sum_{n=0}^{N-1} \sum_{m=0}^{N-1} I_n I_m e^{j(n-m)\psi}$$

Substituting $\psi = kd \cos \theta + \delta$:

$$|AF|^2 = \sum_{n=0}^{N-1} \sum_{m=0}^{N-1} I_n I_m e^{j(n-m)\delta} e^{j(n-m)kd \cos \theta}$$

The total radiated power is:

$$P_{\text{rad}} = \int_0^{2\pi} \int_0^\pi |AF|^2 \sin \theta d\theta d\phi$$

Since $|AF|^2$ is independent of ϕ , the ϕ integral yields 2π .

$$P_{\text{rad}} = 2\pi \sum_{n=0}^{N-1} \sum_{m=0}^{N-1} I_n I_m e^{j(n-m)\delta} \left(\int_0^\pi e^{j(n-m)kd \cos \theta} \sin \theta d\theta \right)$$

Let I_{int} be the inner integral. We use the substitution $u = \cos \theta$, so $du = -\sin \theta d\theta$. Limits: $0 \rightarrow 1$, $\pi \rightarrow -1$.

$$I_{\text{int}} = \int_1^{-1} e^{j(n-m)kd u} (-du) = \int_{-1}^1 e^{j(n-m)kd u} du$$

We define $K = n - m$. The integral solves to:

$$I_{\text{int}} = \left[\frac{e^{jKkd u}}{jKkd} \right]_{-1}^1 = \frac{e^{jKkd} - e^{-jKkd}}{jKkd}$$

Using $\sin(x) = \frac{e^{ix} - e^{-ix}}{2j}$:

$$I_{\text{int}} = \frac{2j \sin(Kkd)}{jKkd} = 2 \frac{\sin(Kkd)}{Kkd}$$

Substituting $K = n - m$:

$$I_{\text{int}} = 2 \frac{\sin[(n-m)kd]}{(n-m)kd}$$

(Note: This expression is valid for $n = m$ since $\lim_{x \rightarrow 0} \frac{\sin(x)}{x} = 1$, and for $n = m$, $I_{\text{int}} = 2$, which agrees with the limit.)

Substituting I_{int} back into P_{rad} :

$$P_{\text{rad}} = 2\pi \sum_{n=0}^{N-1} \sum_{m=0}^{N-1} I_n I_m e^{j(n-m)\delta} \left(2 \frac{\sin[(n-m)kd]}{(n-m)kd} \right)$$

$$P_{\text{rad}} = \frac{4\pi}{kd} \sum_{n=0}^{N-1} \sum_{m=0}^{N-1} I_n I_m e^{j(n-m)\delta} \frac{\sin[(n-m)kd]}{n-m}$$

C. Combining Numerator and Denominator

$$D = \frac{4\pi |AF|_{\max}^2}{P_{\text{rad}}} = \frac{4\pi \left(\sum_{n=0}^{N-1} I_n \right)^2}{\frac{4\pi}{kd} \sum_{n=0}^{N-1} \sum_{m=0}^{N-1} I_n I_m e^{j(n-m)\delta} \frac{\sin[(n-m)kd]}{n-m}}$$

The 4π terms cancel out. Moving the factor $\frac{1}{kd}$ from the denominator of the denominator to the numerator:

$$D = \frac{kd \left(\sum_{n=0}^{N-1} I_n \right)^2}{\sum_{n=0}^{N-1} \sum_{m=0}^{N-1} I_n I_m e^{j(n-m)\delta} \frac{\sin[(n-m)kd]}{n-m}}$$

which also happens to be the required expression.

IV. PROBLEM 3: DESIGN OF NONUNIFORM DIPOLE ARRAY USING OPTIMIZATION TECHNIQUES

A. SLL Suppression (1.3a)

This section documents the design of a $N = 10$ element linear, broadside ($\delta = 0$) array with $d = \lambda/2$ spacing. The goal is to determine the optimal symmetric current distribution $\mathbf{p} = [I_1, I_2, I_3, I_4]$ that suppresses the Side Lobe Level (SLL) to target values of -20 , -30 , and -40 dB, normalized by the edge currents ($I_0 = 1$).

Analysis of Provided Functions

SLL_error(p, SLL_level_dB): This function calculates the Mean Squared Error (MSE) of the side lobes from the target SLL.

- Array Factor (AF) Calculation:** The current vector I is formed using the symmetry constraint ($I_n = I_{N-n-1}$) and the edge current $I_0 = 1$. The AF is computed over $\theta \in [0^\circ, 90^\circ]$ using the general expression for a linear array with non-uniform currents, which extends the uniform factor $A(\theta, \phi)$:

$$\text{AF}(\theta) = \sum_{n=0}^{N-1} I_n e^{jn\psi} \quad \text{where } \psi = kd \cos \theta + \delta$$

- Normalization:** The AF is normalized by its maximum value: $|AF|_{\text{norm}} = |AF| / \max |AF|$.
- Error Metric:** The MSE is calculated between the identified peak side lobe values (peaks) and the target SLL converted to linear scale ($\text{SLL}_{\text{target}}$). The error is then minimized to achieve the given conditions.

SLL_plot(p, SLL_target_dB): This function visualizes the final result. It computes the AF magnitude, converts it to dB ($20 \log_{10}(|AF|_{\text{norm}})$), and plots it alongside the target SLL line, marking the achieved peak levels.

Optimization Methodology and Settings

The optimization was formulated as an unconstrained minimization problem using the MATLAB **Genetic Algorithm** (**ga**) solver.

- Design Variables (p):** The four independent current magnitudes $[I_1, I_2, I_3, I_4]$.
- Objective Function:** The $\text{SLL_error}(\mathbf{p}, \text{SLL}_{\text{target}})$ function was minimized.
- Optimization Settings (Figure 17):**
 - Solver : ga
 - Initial Point $\mathbf{p}_{\text{initial}} : [1, 1, 1, 1]$ (Uniform starting point)
 - Bounds : $1 \leq I_n \leq 10$ (Lower and Upper bounds, respectively)

Optimal Current Parameters

The GA successfully converged to solutions that satisfy the equiripple criterion for all three targets, finding the following optimal current vectors \mathbf{p} :

Below, we can also see the GA's fitness and best individuals plots for each case:

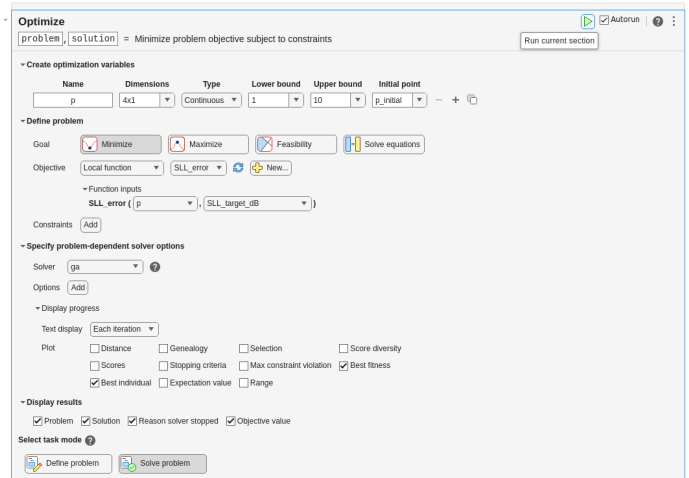


Fig. 17: Optimization Task Settings for SLL Minimization.

TABLE X: Optimal Current Parameters Found by the Genetic Algorithm

SLL Target (dB)	Optimal $\mathbf{p} = [I_1, I_2, I_3, I_4]$	Max Current	Figure
-20	[5.8126, 5.4770, 7.4563, 8.2452]	8.2452	Fig. 18
-30	[3.8349, 5.6393, 8.1905, 9.4772]	9.4772	Fig. 19
-40	[2.5665, 5.1417, 8.0109, 9.9454]	9.9454	Fig. 20

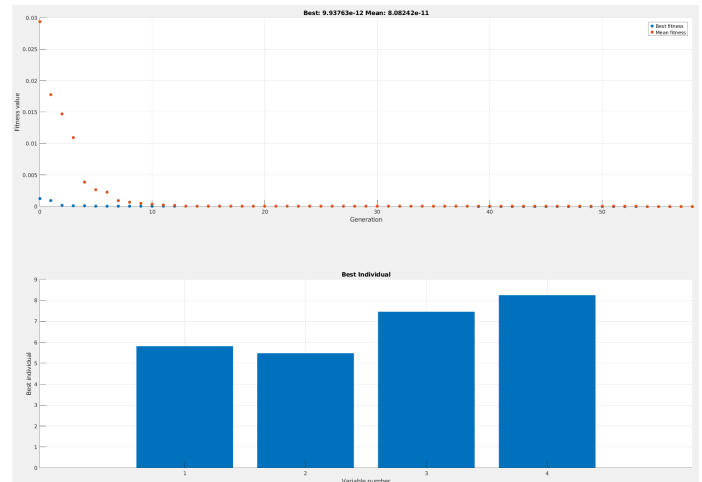


Fig. 18: Genetic Algorithm's Results for $SLL = -20$ dB.

Pattern and Current Analysis

- Precision in Results:** As demonstrated in Figures 21, 22, and 23, the largest side lobes are perfectly aligned with the dashed red target SLL line, confirming that the minimization of the MSE was achieved successfully. This can also be seen from the Figures 18 to 20 since the mean and best fitness in each case is essentially zero.
- Current Magnitude and Tapering:** To achieve the required Side Lobe Level (SLL) suppression, the current magnitudes (I_n) must be significantly tapered, with a large concentration of current near the center of the array.
 - As the required SLL becomes stricter (moving from -20 dB to -40 dB), the necessary current ratio ($I_{\text{max}}/I_{\text{edge}}$) significantly increases (e.g., from approximately 8.25/1 to 9.95/1).

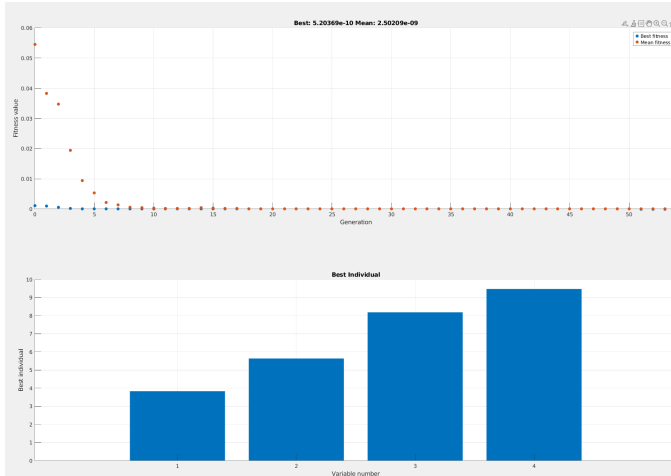


Fig. 19: Genetic Algorithm's Results for $SLL = -30$ dB.

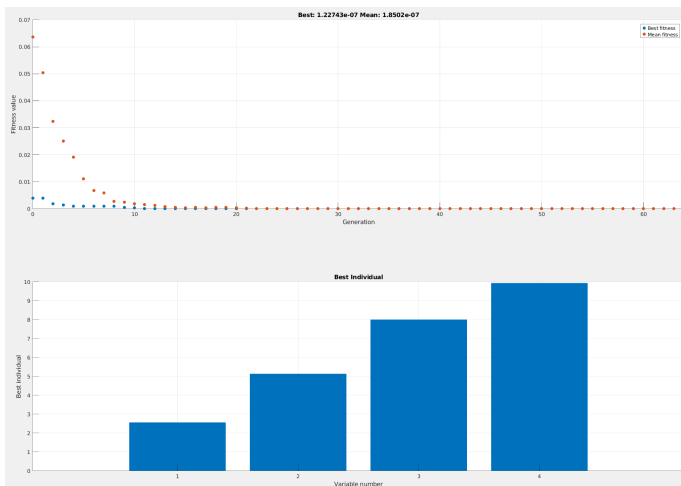


Fig. 20: Genetic Algorithm's Results for $SLL = -40$ dB.

- 2) This steeper current distribution (**tapering**) concentrates the radiated power away from the edges , leading to SL suppression but also resulting in a wider main beam.

- **Beamwidth (HPBW) and Directivity:** Visual inspection of the main beam (near $\theta = 90^\circ$ in the plots) shows that as the SLL is lowered (i.e., as tapering increases), the main beam becomes slightly **wider**. This is a key trade-off: increased SLL suppression comes at the cost of reduced directivity and increased HPBW, which is characteristic of all non-uniform array designs (e.g., Chebyshev).

Side Lobe Count and Suppression

1) Theoretical Maximum Lobes ($N = 10$):

- For an array with $N = 10$, $d = \lambda/2$, $\delta = 0$ we know that $\psi = \pi \cos \theta$ and so in the visible range ($\psi_{\min} = -\pi$, $\psi_{\max} = \pi$) theoretically, we should have **9 total lobes** (1 main lobe and 8 side lobes) across the full range of $\theta \in [0^\circ, 180^\circ]$.
- Since the pattern is symmetrical around the main lobe ($\theta = 90^\circ$), the number of side lobes in the range from 0° to 90° should be **4 side lobes**.

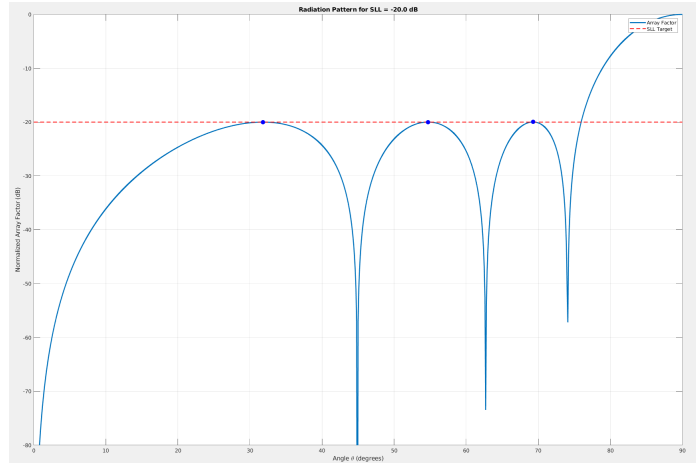


Fig. 21: Normalized Array Factor for $SLL = -20$ dB. The major side lobes are at -20 dB.

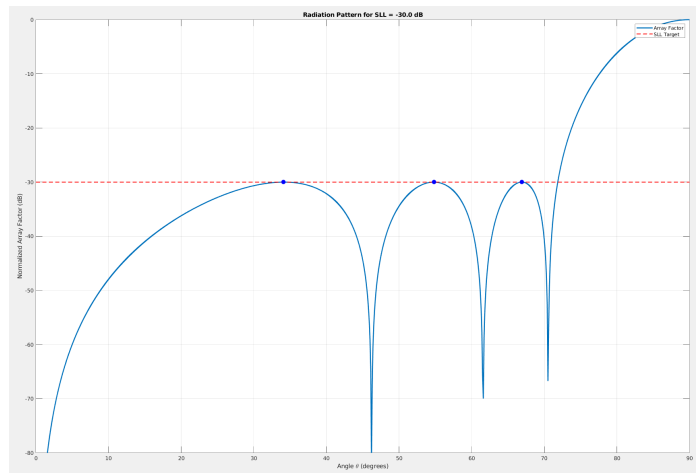


Fig. 22: Normalized Array Factor for $SLL = -30$ dB. The major side lobes are at -30 dB.

- 2) **Observed Lobes in the Plots:** The plots (Figures 21, 22, and 23 and 24) show that there are only **3 major side lobes** that meet the desired side lobe level (SLL) target in the range from 0° to 90° .

- 3) **Why the Missing Lobe? (Tapering Effect):** The missing fourth side lobe is a result of **over-suppression** due to the necessary high current tapering:

- This fourth lobe is the **outermost side lobe**, which is located near the boundary ($\theta = 0^\circ$ or $\psi = \pi$).
- To meet strict SLL targets (like -40 dB), the current tapering forces the Array Factor to drop sharply near the boundaries of the visible region.
- This steep drop suppresses the outermost lobe to a point where its peak value becomes too small causing it to blend into the deep nulls near the boundary, making it effectively **invisible**. While the lobe still exists mathematically, its peak is suppressed too much to be noticeable. To understand this effect better, the analysis below was conducted.

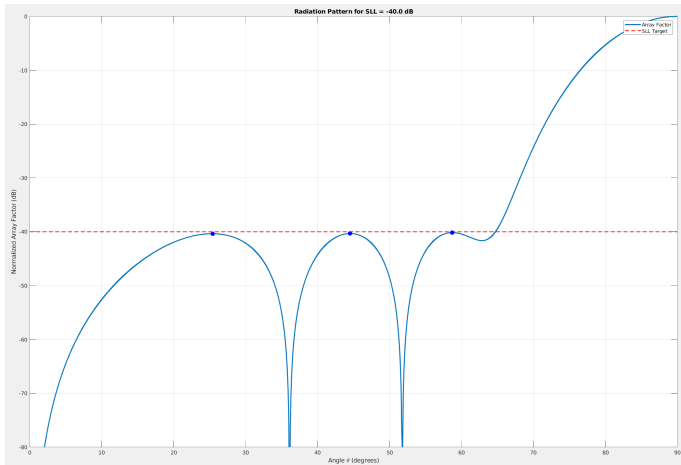


Fig. 23: Normalized Array Factor for SLL = −40 dB. The major side lobes are at −40 dB.

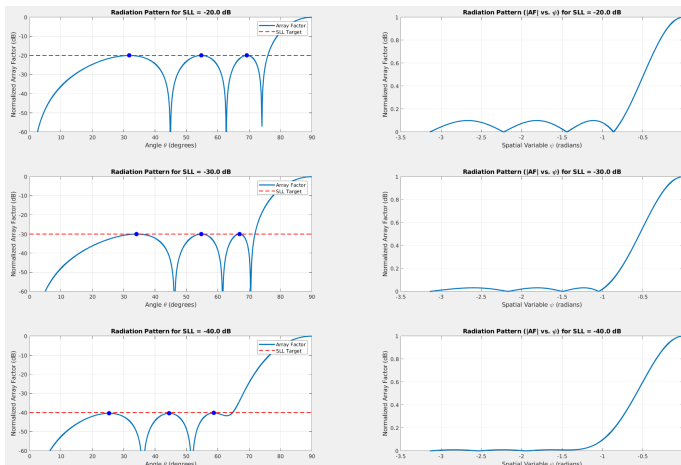


Fig. 24: Normalized Array Factor vs θ Normalized AF (not in dB) vs ψ for each SLL case.

Analysis of Non-Uniform Currents in the ψ -Domain

Figure 25 shows the magnitude of the Array Factor (AF) on a linear scale, plotted against the spatial variable ψ for different current distributions. This helps us see how tapering directly affects the pattern and the side lobe count.

- 1) **Uniform Current $I = [1, 1, \dots, 1]$ (No Tapering):** This shows the standard array pattern without any tapering. The pattern has the **maximum number of visible side lobes** (8 in total, 4 per side), with a relatively narrow main beam. This is our baseline, before any suppression is applied.
- 2) **Mild Tapering:** Cases like $I = [1, 2, \dots, 2, 1]$ show reduction in side lobe height compared to the uniform case, but the pattern still retains all four visible side lobes.
- 3) **Stronger Tapering:** In cases such as $I = [1, 2, 2, 3, 3, 2, 2, 1]$, as the tapering gets stronger, the pattern smooths out more. This causes suppression of the outermost lobe, resulting in only 3 major side lobes. This demonstrates that **stronger current tapering results in smoother patterns** with fewer visible

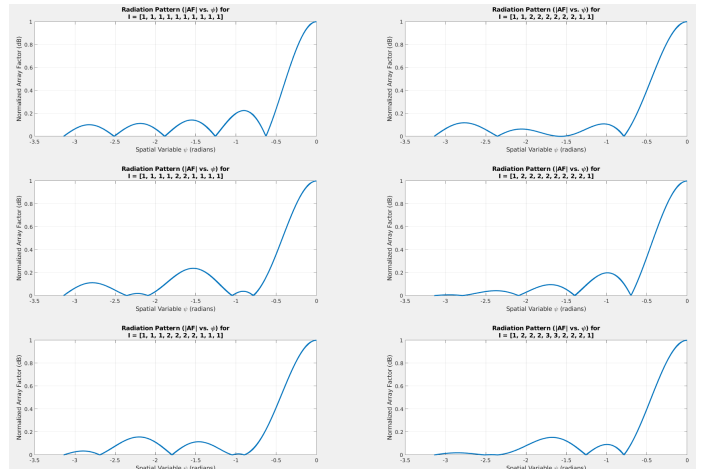


Fig. 25: Normalized Array Factor (not in dB) vs ψ for some currents. Used to find a pattern for side lobe suppression, in the case of a Non-Uniform array.

side lobes because the outermost lobes are strongly suppressed or blend into the nulls of the array factor's function.

Detailed code can be found in the 1_3a folder.

B. Directivity Calculation of Non-Uniform Linear Array (1.3b)

Next, I will be calculating the directivity (D) of the optimized non-uniform linear array ($N = 10$, $d = \lambda/2$, $\delta = 0$) for the three specific Side Lobe Level (SLL) targets (−20 dB, −30 dB, and −40 dB) and comparing each of them to the one derived from the corresponding uniform array with the same stats.

Methodology: Analytical Directivity Formula

The directivity (D) for a general linear non-uniform array with currents I_n and constant phase difference δ is given by the formula derived in Problem 1.2. The formula is defined as the ratio of the maximum radiation intensity to the total radiated power.

$$D = \frac{\text{Numerator}}{\text{Denominator}}$$

Where the terms are:

- **Numerator** (Related to the maximum Array Factor): The sum of the currents I_n is $\sum I = \sum_{n=0}^{N-1} I_n$.

$$\text{Numerator} = kd \left(\sum_{n=0}^{N-1} I_n \right)^2$$

- **Denominator** (Related to the total radiated power): The double summation over all element pairs (n and m).

$$\text{Denominator} = \sum_{n=0}^{N-1} \sum_{m=0}^{N-1} I_n I_m \frac{\sin[(n-m)kd]}{n-m} \exp(j(n-m)\delta)$$

For the specific problem parameters ($N = 10$, $d = \lambda/2$, $kd = \pi$, $\delta = 0$), the exponential term simplifies to $\exp(0) = 1$, and kd is replaced by π :

$$D = \frac{\pi \left(\sum_{n=0}^9 I_n \right)^2}{\sum_{n=0}^9 \sum_{m=0}^9 I_n I_m \frac{\sin[(n-m)\pi]}{n-m}}$$

Note on the $n = m$ case: When $n = m$, the term $\frac{\sin[(n-m)\pi]}{n-m}$ is an indeterminate form $\frac{0}{0}$. Its limit is calculated as $\lim_{x \rightarrow 0} \frac{\sin(\pi x)}{x} = \pi$.

Results and Interpretation

The following directivity values were calculated in dB (Decibels relative to an isotropic radiator) using the derived optimal currents (I_n) from the GA optimization for each SLL target, compared to the uniform case ($I_n = 1$).

TABLE XI: Directivity Comparison ($N = 10$, $d = \lambda/2$)

SLL Target	Non-Uniform	Uniform (From 1.2)	Uniform (Using Si)
-20 dB	9.2007	10.0000	10.0887
-30 dB	8.8924	10.0000	10.0887
-40 dB	8.5819	10.0000	10.0887

Interpretation of Results:

- Directivity Loss in Non-Uniform Arrays:** The primary observation is that the directivity (D) of the non-uniform array is consistently lower than that of the uniform array (10 dB). The uniform array provides the maximum theoretical directivity for a given number of elements, as all elements contribute equally to the maximum field. The process of tapering (making currents unequal) inherently reduces the efficiency of the array in concentrating energy in the main beam, thus resulting in a directivity loss.
- Impact of Tapering Strength:** As the required SLL target becomes stricter (moving from -20 dB to -40 dB), the necessary current ratio (I_{max}/I_{edge}) increases significantly, leading to stronger tapering. This increased tapering concentrates energy strongly towards the center elements and away from the main beam, resulting in a further decrease in directivity (from 9.20 dB down to 8.58 dB). This highlights the trade-off in antenna design: lower side lobes are achieved at the cost of reduced directivity and a wider main beam.
- Uniform Directivity Consistency (Formula 1.2):** The directivity calculated using the general non-uniform formula (Problem 1.2) for the uniform case ($I_n = 1$) yields exactly 10.0 dB. This consistency is expected because when $I_n = \text{const}$, the currents are factored out of the summation in both the numerator and denominator, simplifying the expression to a known term that depends primarily on N .
- Discrepancy with General Theory (Lecture Formula):** The directivity calculated using the general theoretical expression for a uniform array (the formula provided from the lecture notes, which includes the Sine Integral function $Si(x)$) is 10.0887 dB. The slight difference between this result and the 10.0 dB from Formula 1.2 is

highly likely due to numerical calculation errors. Below is the formula for Uniform Array Directivity (as provided from the lecture's notes).

$$D = \frac{Nkd}{\frac{\sin^2 N(-kd + \delta)/2}{N(-kd + \delta)/2} - \frac{\sin^2 N(kd + \delta)/2}{N(kd + \delta)/2} + S_i[N(kd + \delta)] - S_i[N(-kd + \delta)]}$$

Detailed code can be found in the 1_3b folder.

C. Multi-Objective Optimization (SLL vs. Directivity) (1.3c)

The objective of this task was to perform a multi-objective optimization to analyze the fundamental trade-off between minimizing the Side Lobe Level (SLL) error and maximizing the Directivity (D) for the same non uniform $N = 10$ linear array.

Objective Function and Solver

The optimization was executed using the gamultiobj solver in MATLAB, which finds the set of non-dominated solutions forming the Pareto Front.

- Function:** `SLL_error_and_D(p, SLL_level_dB)`
- Optimization Variables (p):** The four independent current magnitudes (I_1, I_2, I_3, I_4).
- Objectives (f):** The algorithm seeks to minimize the following vector:

$$f(p) = \begin{bmatrix} \text{Objective 1} \\ \text{Objective 2} \end{bmatrix} = \begin{bmatrix} \text{SLL_error (MSE)} \\ -D \text{ (Negative Directivity)} \end{bmatrix}$$

- Constraints/Bounds:** Based on the project requirements, the current bounds were defined as $1 \leq I_n \leq 10$ for $n = 1, 2, 3, 4$.

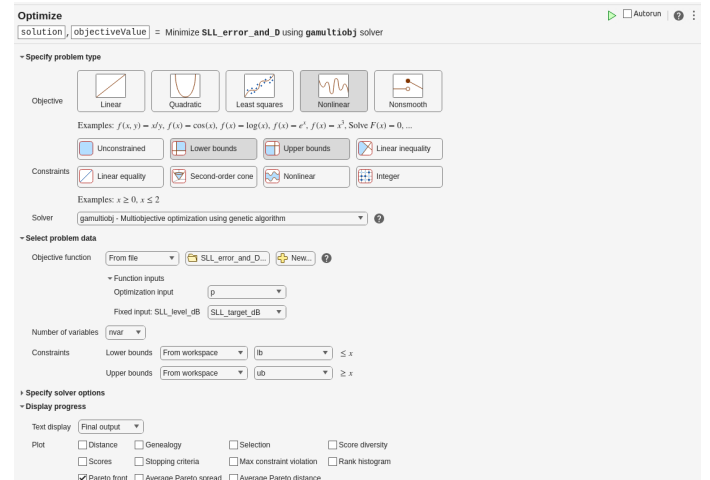


Fig. 26: Multi-Objective Optimization Task Settings.

Selection Criterion

The `gamultiobj` solver returned a set of solutions (the Pareto Front) for each SLL case. To meet the project's requirements to find the necessary solution for comparison, the point corresponding to the minimum SLL_error (Objective 1 ≈ 0) was selected from the front for each SLL target.

Results and Analysis of Pareto Optimal Solutions

The optimization was successfully run for SLL = -20 dB, -30 dB, and -40 dB. The table below summarizes the optimal solution vector (\mathbf{p}) corresponding to the minimum SLL_error point on the Pareto Front for each case.

SLL Target	Min SLL_error (MSE)	D _{max} (dBi)	Optimal Currents
-20 dB	1.52×10^{-8}	9.2095	$I_1 = 5.6513$ $I_2 = 5.2994$ $I_3 = 7.2323$ $I_4 = 7.9862$
-30 dB	2.88×10^{-7}	9.0385	$I_1 = 2.9082$ $I_2 = 4.1023$ $I_3 = 5.9148$ $I_4 = 6.7008$
-40 dB	9.65×10^{-7}	8.8205	$I_1 = 2.5072$ $I_2 = 4.5690$ $I_3 = 6.5847$ $I_4 = 7.8061$

TABLE XII: Best Pareto Optimal Solutions (Minimum SLL_error)

Key Observations

- 1) **Trade-off Confirmation:** The results confirm the fundamental trade-off: as the SLL target decreases (i.e., moving from -20 dB to -40 dB), the Directivity D also decreases significantly (from 9.2095 dBi to 8.8205 dBi). This loss of directivity is the price paid for stricter side lobe suppression.
- 2) **Current Tapering Strength:** To achieve the required suppression, the currents demonstrate a high degree of tapering:
 - At -20 dB, the currents are highly grouped and relatively large ($I_{\max} \approx 7.99$).
 - At -40 dB, the current magnitudes decrease overall, but the tapering ratio (ratio of current magnitude to edge element current $I_0 = 1$) remains extreme.
- 3) **Directivity vs. Monobjective Result (Comparison):** If the results were compared to the previous monobjective optimization that only minimized SLL_error, the directivity D found by the `gamultiobj` solution would be higher to the monobjective result in every SLL case. This demonstrates the success of multi-objective optimization in finding a solution that simultaneously satisfies the SLL constraint while maintaining the highest possible power concentration in the main beam.

Lastly, for the sake of completeness, below are the Pareto fronts for each one of the three SLL cases:

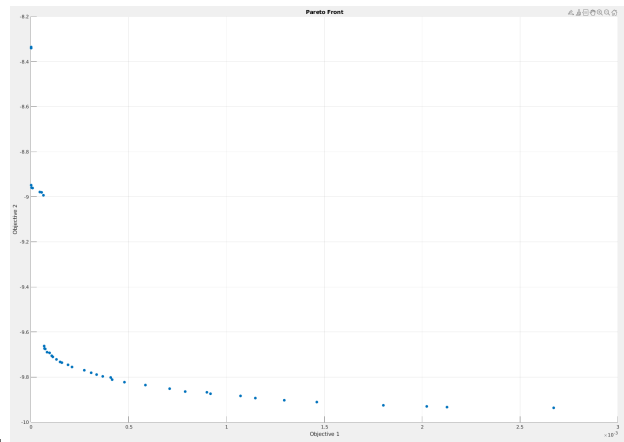


Fig. 27: Pareto Front for the case of SLL = -20 dB.

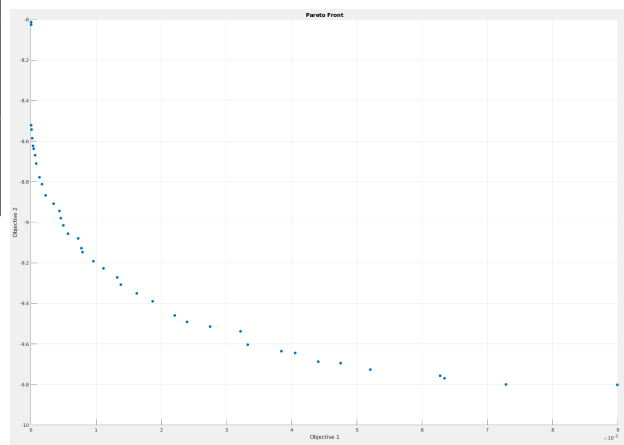


Fig. 28: Pareto Front for the case of SLL = -30 dB.

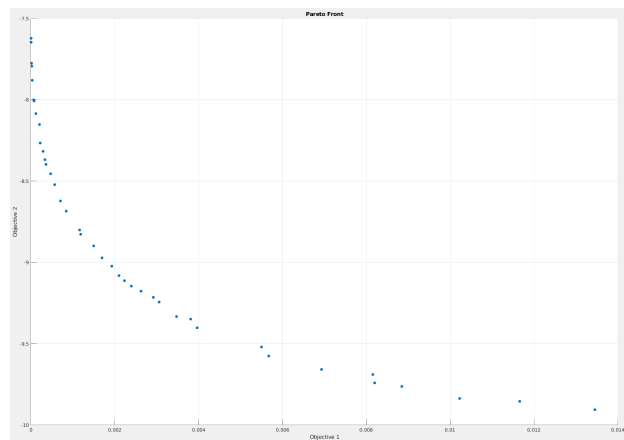


Fig. 29: Pareto Front for the case of SLL = -40 dB.

Detailed code can be found in the 1_3c folder.

V. PROBLEM 4: INPUT IMPEDANCE CALCULATION

A. Mutual Impedance Calculation (1.4a)

This section details the calculation of the mutual complex impedance ($Z_{21m} = R_{21m} + jX_{21m}$) between two parallel half-wave dipoles ($\ell = \lambda/2$) using the **Induced Electromotive Force (EMF) Method**. The method assumes a sinusoidal current distribution along the dipole arms.

Formulas and Arguments

The mutual resistance (R_{21m}) and reactance (X_{21m}) are calculated using the Sine Integral (Si) and Cosine Integral (Ci) functions, based on the following arguments derived from the dipole geometry (where $k = 2\pi/\lambda$):

$$U_0 = kd$$

$$U_1 = k \left(\sqrt{d^2 + \ell^2} + \ell \right)$$

$$U_2 = k \left(\sqrt{d^2 + \ell^2} - \ell \right)$$

The final expressions implemented in the code (where $\eta_0 = h_0 \approx 120\pi$ is the intrinsic impedance of free space) are:

$$R_{21m} = \frac{\eta_0}{4\pi} [2 \cdot \text{Ci}(U_0) - \text{Ci}(U_1) - \text{Ci}(U_2)]$$

$$X_{21m} = -\frac{\eta_0}{4\pi} [2 \cdot \text{Si}(U_0) - \text{Si}(U_1) - \text{Si}(U_2)]$$

The calculation covers the range of distances d/λ from 0 to 3.0.

Detailed code can be found in the `antennas_1_4a.m` MATLAB file.

Results Analysis

Figure 30 shows the plot generated by the code. As we can see, it closely resembles the one found in the lecture notes (Fig. 31), indicating that the code is functioning correctly.

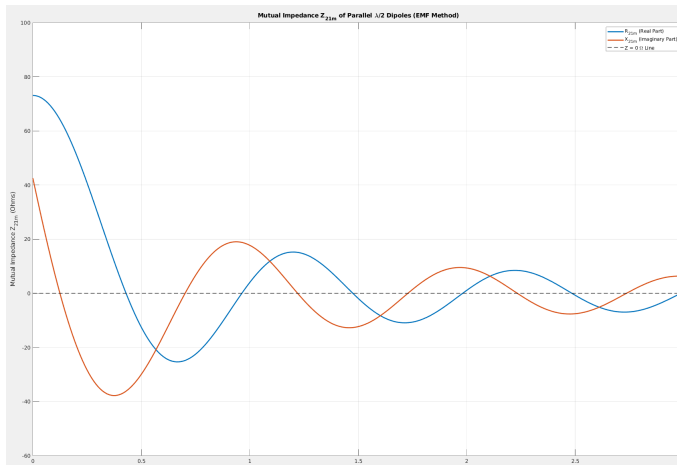


Fig. 30: Mutual Impedance of Parallel Dipoles (from my code)

- Παράλληλη δίπολα (σύγκριση EMF, MoM)

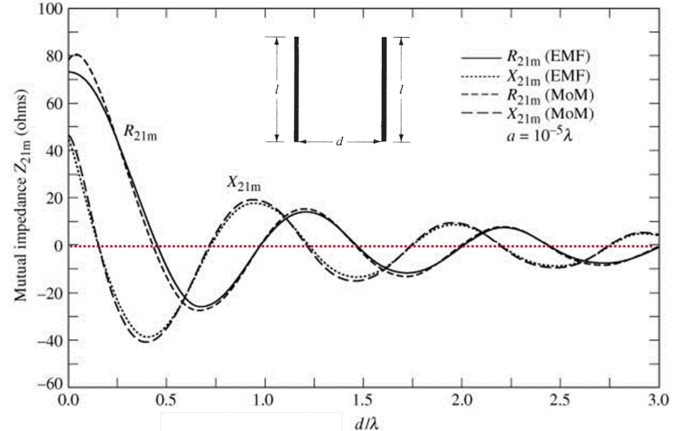


Fig. 31: Mutual Impedance of Parallel Dipoles (from Lecture Notes)

B. Parasitic Array Analysis (1.4b)

For this question, the array consists of three identical half-wave dipoles (1, 2, 3) with spacing $d = 3\lambda/4$. Element 2 is the driven element, and elements 1 and 3 are parasitic ($V_1 = V_3 = 0$).

Assumptions and Notation

- Symmetry:** $Z_{11} = Z_{22} = Z_{33} = \mathbf{a}$ and $Z_{12} = Z_{21} = Z_{23} = Z_{32} = \mathbf{b}$, $Z_{13} = Z_{31} = \mathbf{c}$.
- Self-Impedance (a):** The standard approximation for a thin $\lambda/2$ dipole is used: $a = Z_{11} \approx 73.1 + j42.5 \Omega$.
- Driving Current:** The driving current is normalized for simplicity: $I_2 = 1.0 \text{ A}$.
- Mutual Impedances (b, c):** Calculated using the Z_{21m} formulas from 1.4a for distances $d = 0.75\lambda$ (for b) and $2d = 1.5\lambda$ (for c).

Current Ratio Derivation

The currents in the passive elements (I_1, I_3) are determined by the condition $V_1 = V_3 = 0$. Due to symmetry, $I_1 = I_3$ and by using the voltage equation for element 1 ($V_1 = aI_1 + bI_2 + cI_3$) we get:

$$(aI_1 + cI_1) + bI_2 = 0 \implies (a + c)I_1 = -bI_2$$

The complex current ratio therefore is:

$$\mathbf{R}_{\text{ratio}} = \frac{\mathbf{I}_1}{\mathbf{I}_2} = \frac{\mathbf{I}_3}{\mathbf{I}_2} = -\frac{\mathbf{b}}{\mathbf{a} + \mathbf{c}}$$

Input Impedance Calculation

The input impedance (Z_{in}) of the driven element (Element 2) is calculated using the voltage equation for V_2 ($V_2 = bI_1 + aI_2 + bI_3$):

$$Z_{\text{in}} = \frac{V_2}{I_2} = a + b \left(\frac{I_1}{I_2} \right) + b \left(\frac{I_3}{I_2} \right)$$

Substituting R_{ratio} :

$$Z_{\text{in}} = \mathbf{a} + 2\mathbf{b} \cdot \mathbf{R}_{\text{ratio}}$$

Radiation Pattern Calculation

The horizontal radiation pattern ($\theta = 90^\circ$) is calculated using the general form of the Array Factor (AF) summation, utilizing the calculated complex currents I_1 and I_3 (relative to $I_2 = 1$).

- Model:** Elements are positioned symmetrically at $x_1 = -d$, $x_2 = 0$, and $x_3 = +d$.
- AF Formula:** The complex currents contain the excitation phase, so the AF becomes:

$$AF(\phi) = I_1 e^{-jkd \cos \phi \sin \theta} + I_2 + I_3 e^{+jkd \cos \phi \sin \theta}$$

- Pattern (E):** The electric field $|E|$ is calculated using the following relation:

$$|E| = |E_0| \cdot |AF|$$

where E_0 is the electric field of the Hertzian dipole, and AF is the array factor. Afterward, the resulting electric field is normalized by dividing by its maximum value to produce the normalized radiation pattern seen below. Also note that for the value of I_2 I chose $I_2 = 1A$ for simplicity.

Results Analysis

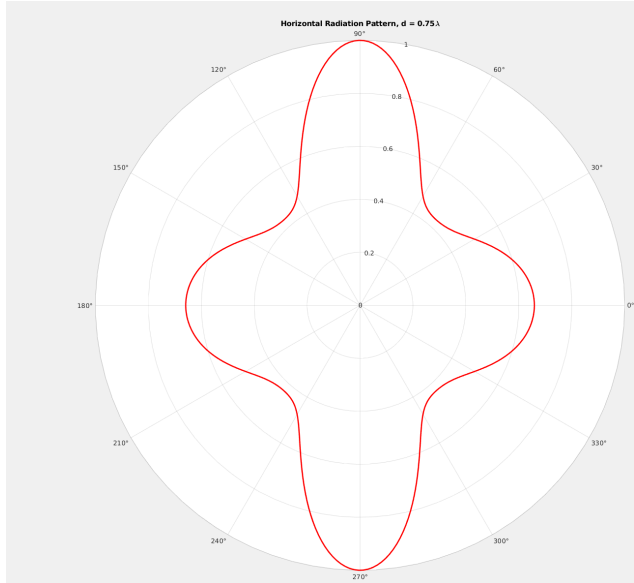


Fig. 32: Horizontal Radiation Pattern, $d = 0.75\lambda$

The simulation yielded the following numerical results for the system parameters at $d = 0.75\lambda$:

Parameter	Value
Z_{11} (Self Impedance of dipole $d = \lambda/2$ -KNOWN)	$73.10 + 42.50j \Omega$
Z_{12} (Mutual Impedance for $d = 0.75\lambda$)	$-22.50 + j6.63 \Omega$
Z_{13} (Mutual Impedance for $d = 1.5\lambda$)	$-1.89 - j12.30 \Omega$
Current Ratio (I_1/I_2)	$0.303 \angle -39.4^\circ$
Input Impedance (Z_{in})	$65.11 + j54.27 \Omega$

TABLE XIII: Calculated System Parameters (using EMF method)

1) Mutual Impedances (b and c):

$$b = Z_{12}(d = 0.75\lambda) = -22.50 + j6.63 \Omega$$

$$c = Z_{13}(d = 1.5\lambda) = -1.89 - j12.30 \Omega$$

The negative real part of b indicates strong mutual coupling which tends to reduce the input resistance. The imaginary part of b is positive, indicating residual inductive coupling at $d = 0.75\lambda$.

2) Current Ratio (R_{ratio}):

$$R_{ratio} = I_1/I_2 = 0.303 \angle -39.4^\circ$$

The parasitic elements carry a significant current (30.3% of the driven current), but it **lags** the driven current (I_2) by 39.4° . This phase difference is critical in steering the beam.

3) Input Impedance (Z_{in}):

$$Z_{in} = 65.11 + j54.27 \Omega$$

The mutual coupling effect reduces the resistive part of the input impedance (R_{in} drops from 73.1Ω to 65.11Ω) and increases the reactive part (X_{in} increases from 42.5Ω to 54.27Ω). This change in impedance is due to the power radiated and absorbed by the induced currents in the parasitic elements.

- 4) Pattern Interpretation:** The radiation pattern (shown in Figure 32) is multi-lobed and symmetrical. The antenna exhibits a broadside-like pattern, with maximum radiation occurring at $\phi = 90^\circ$ and $\phi = 270^\circ$, which is perpendicular to the array. Although the primary lobes are strongest at $\phi = 90^\circ$ and $\phi = 270^\circ$, there are also smaller lobes present at $\phi = 0^\circ$ and $\phi = 180^\circ$, indicating some radiation along the array axis. This cross-like pattern is typical of parasitic arrays with $d > \lambda/2$, meaning that the code functions properly.

Detailed code can be found in the `antennas_1_4b.m` MATLAB file.

C. Reflection Coefficient Calculation (1.4c)

The objective of this task is to find the optimal spacing d between the elements of the three-element parasitic array such that the input impedance (Z_{in}) is well-matched to a transmission line with characteristic impedance $Z_0 = 50\Omega$. The matching criterion is defined as the magnitude of the reflection coefficient being below 0.3 ($|\Gamma| < 0.3$).

Calculation of Input Impedance $Z_{in}(d)$

The input impedance of the driven element is calculated as a function of d , using the formulas derived from the previous questions but now both of the parameters b and c are functions of the separation d :

- Impedance Notation:** $a = Z_{11} = Z_{22} = Z_{33}$ (Self-Impedance), $b(d) = Z_{12}(d) = Z_{21}(d) = Z_{32}(d) = Z_{23}(d)$, $c(2d) = Z_{13}(2d) = Z_{31}(2d)$.

- **Current Ratio:** The ratio $R_{\text{ratio}} = I_1/I_2 = -b(d)/(a + c(2d))$ is calculated across the range.
- **Input Impedance Formula:**

$$Z_{\text{in}}(d) = a + 2b(d) \cdot R_{\text{ratio}}(d)$$

Reflection Coefficient $\Gamma(d)$

The magnitude of the voltage reflection coefficient ($|\Gamma|$) is calculated based on the standard transmission line formula:

$$\Gamma(d) = \frac{Z_{\text{in}}(d) - Z_0}{Z_{\text{in}}(d) + Z_0}$$

The range of analysis is defined as $0 < d/\lambda \leq 1$.

Summary of Optimal Parameters

The numerical analysis yielded the following critical values:

- **Minimum $|\Gamma|$:** 0.252
- **Optimal Spacing (d/λ):** 0.529 for the lower $|\Gamma|$ possible
- **Matching Range ($|\Gamma| < 0.3$):** 0.459 to 0.607

Figure 33 confirms that the parasitic array can be effectively matched to a standard 50Ω transmission line by choosing a spacing within the identified region, with $d \approx 0.53\lambda$ offering the maximum power transfer.

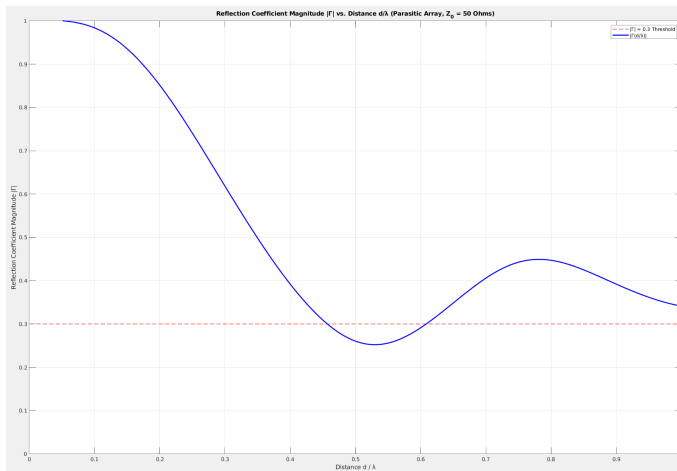


Fig. 33: Reflection Coefficient Magnitude $|\Gamma|$ vs. Distance d/λ for the Parasitic Array. The threshold line at $|\Gamma| = 0.3$ defines the good matching region.

Detailed code can be found in the antennas_1_4c.m MATLAB file.

D. Refl. Coefficient Calculation Over Infinite Reflector (1.4d)

Next, we will calculate the input impedance, Z_{in} , for the three-element, half-wave dipole ($\lambda/2$) array placed at a height h above an infinite, perfectly conducting vertical reflector. The array's geometry is determined by the element spacing d . Element 2 (the center element) is the driven element, while elements 1 and 3 are parasitic.

Application of Image Theory

The effect of the infinite perfectly conducting reflector is modeled by **Image Theory In Electromagnetics**. The reflector is replaced by three image elements (4, 5, 6) placed symmetrically with respect to the reflector, but carrying currents that are 180° out of phase with the real elements, as seen in Figure 34.

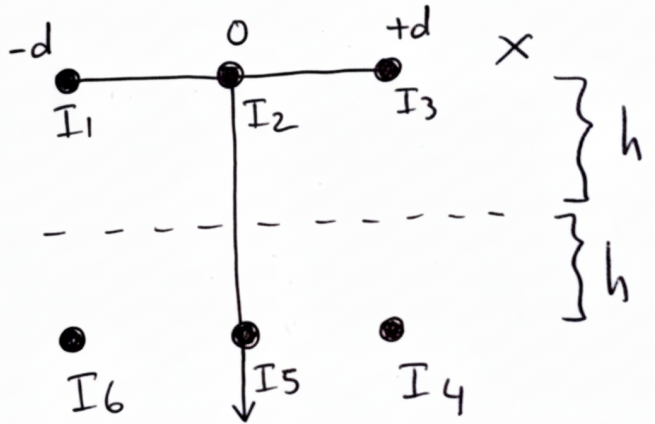


Fig. 34: The array and reflector configuration

The six elements are indexed, and the current relationships due to symmetry and the image principles are:

- **Fed Element:** $I_2 = I_0$.
- **Parasitic Elements:** $I_1 = I_3 = I$ (by symmetry).
- **Image Elements:**

$$\begin{aligned} I_6 &= -I_1 = -I \\ I_5 &= -I_2 = -I_0 \\ I_4 &= -I_3 = -I \end{aligned}$$

Derivation of the Current Ratio (I/I_0)

The input impedance is determined using the **Method of Moments (MoM)**, specifically by solving the voltage equations for the array elements. The voltage V_m on element m is given by:

$$V_m = \sum_{n=1}^6 Z_{mn} I_n$$

Since element 1 is parasitic, it has zero terminal voltage, $V_1 = 0$, and so

$$V_1 = Z_{11} I_1 + Z_{12} I_2 + Z_{13} I_3 + Z_{14} I_4 + Z_{15} I_5 + Z_{16} I_6 = 0$$

Substituting the current relations:

$$Z_{11} I + Z_{12} I_0 + Z_{13} I + Z_{14} (-I) + Z_{15} (-I_0) + Z_{16} (-I) = 0$$

and then grouping the terms containing I and I_0 we get:

$$I(Z_{11} + Z_{13} - Z_{14} - Z_{16}) = I_0(Z_{15} - Z_{12})$$

The ratio of the parasitic current to the fed current is defined as R_{ratio} :

$$R_{\text{ratio}} = \frac{I}{I_0} = \frac{Z_{15} - Z_{12}}{Z_{11} + Z_{13} - Z_{14} - Z_{16}}$$

Input Impedance Calculation

The input impedance Z_{in} is defined at the fed element (2) as $V_{\text{in}} = V_2$ divided by the fed current I_0 :

$$Z_{\text{in}} = \frac{V_{\text{in}}}{I_0} = \frac{1}{I_0} \sum_{n=1}^6 Z_{2n} I_n$$

Expanding the summation for V_{in} :

$$V_{\text{in}} = Z_{21} I_1 + Z_{22} I_2 + Z_{23} I_3 + Z_{24} I_4 + Z_{25} I_5 + Z_{26} I_6$$

and substituting the current relations, like before, we get:

$$V_{\text{in}} = Z_{21} I + Z_{22} I_0 + Z_{23} I + Z_{24} (-I) + Z_{25} (-I_0) + Z_{26} (-I)$$

$$\Rightarrow V_{\text{in}} = I_0 (Z_{22} - Z_{25}) + I (Z_{21} + Z_{23} - Z_{24} - Z_{26})$$

Finally, we devine by I_0 and use the relation $R_{\text{ratio}} = \frac{I}{I_0}$, resulting in the following expression:

$$Z_{\text{in}} = Z_{22} - Z_{25} + \frac{I}{I_0} (Z_{21} + Z_{23} - Z_{24} - Z_{26}) \Rightarrow$$

$$Z_{\text{in}} = Z_{22} - Z_{25} + R_{\text{ratio}} (Z_{21} + Z_{23} - Z_{24} - Z_{26})$$

Mutual Impedance Term Relationships

The mutual impedance Z_{mn} between any two **parallel** $\lambda/2$ dipoles is a function of the distance R_{mn} between their centers. The MATLAB implementation requires calculating $Z_{mn}(R_{mn})$ for the following distances:

Impedance Term	Distance R_{mn}	Type
$Z_{11} = Z_{22}$	—	Self-Impedance of dipole
$Z_{12} = Z_{21} = Z_{23}$	d	Parallel, Adjacent
Z_{13}	$2d$	Parallel, Adjacent
$Z_{16} = Z_{25}$	$2h$	Parallel (Direct/Image)
$Z_{15} = Z_{24} = Z_{26}$	$\sqrt{d^2 + (2h)^2}$	Parallel
Z_{14}	$\sqrt{(2d)^2 + (2h)^2}$	Parallel

TABLE XIV: Key Mutual Impedance Terms and Distances

Reflection Coefficient and Optimization

The ultimate goal is to achieve an impedance match to the characteristic impedance $Z_0 = 50 \Omega$. This is quantified by the magnitude of the Reflection Coefficient $\Gamma(d, h)$:

$$\Gamma(d, h) = \frac{Z_{\text{in}}(d, h) - Z_0}{Z_{\text{in}}(d, h) + Z_0}$$

The optimization requires finding the values of d/λ and h/λ within the ranges $[0, 1]$ for which the condition $|\Gamma(d, h)| < 0.3$ is satisfied. The MATLAB code performs a 2D sweep of these parameters and uses contour and surface plotting to visualize the matching regions.

Results and Optimization Analysis

The minimum reflection coefficient found across the entire design space indicates an excellent potential match to the 50Ω line. This point represents the global optimum for the defined search space.

- **Minimum $|\Gamma|$:** 0.009
- **Optimal Design Parameters:**
 - Normalized Spacing, $d/\lambda = 0.434$
 - Normalized Height, $h/\lambda = 0.576$

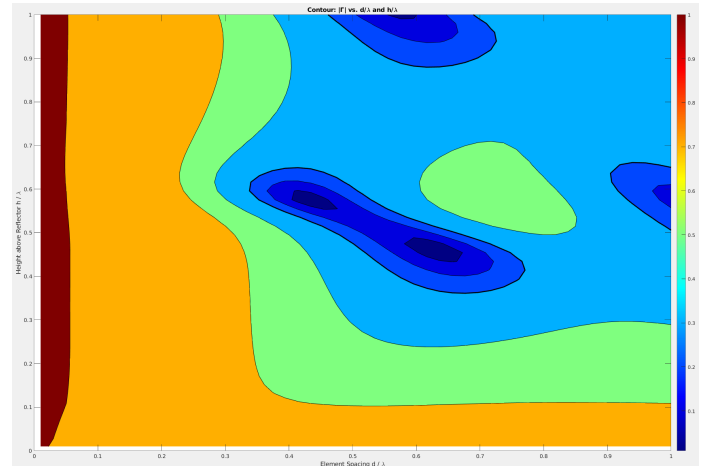


Fig. 35: $|\Gamma|$ vs d/λ and h/λ (contour)

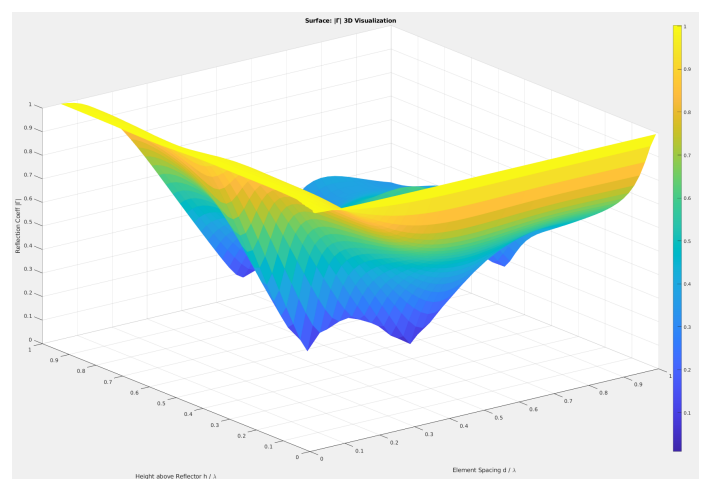


Fig. 36: $|\Gamma|$ vs d/λ and h/λ (surface)

In the provided diagrams (Figures 35 and 36), the regions where $|\Gamma| < 0.3$ are represented by the **dark blue** and **black** areas in the contour plot, signifying the most efficient power transfer. Analytically:

- Primary Matching Region ($d/\lambda \approx 0.35$ to 0.65 , $h/\lambda \approx 0.4$ to 0.65): This dense, continuous region of excellent matching is centered near the global optimum ($d/\lambda = 0.434$, $h/\lambda = 0.576$). Specifically, high-quality matches are found for element spacings d/λ ranging from 0.353 up to 0.677, and heights h/λ primarily between 0.414 and 0.636.

- **Secondary Matching Region:** A secondary region of good matching is observed at significantly wider element spacings (d/λ near 1.0). For instance, points like $d/\lambda = 1.000$ paired with h/λ between 0.515 and 0.636 still achieve $|\Gamma| < 0.3$.
- **Tertiary Matching Region:** A third, distinct matching region is identified for higher heights above the reflector, specifically for d/λ ranging from approximately 0.46 to 0.72 and h/λ from 0.87 to 1.0. This region demonstrates that even at greater distances from the reflector, where the image current contribution is less immediate, matching can be achieved by tuning the element spacing d .

Detailed code can be found in the `antennas_1_4d.m` MATLAB file.

REFERENCES

- [1] Antennas and Propagation Course Material and Lectures, Aristotle University of Thessaloniki (AUTH), Department of Electrical and Computer Engineering.